IGNITION OF CHARCOAL ADSORBERS BY FISSION PRODUCT DECAY HEAT*

R. P. Shields

Reactor Chemistry Division, Oak Ridge National Laboratory, Oak Ridge, Tenn.

ABSTRACT

The problem of estimating maximum temperatures in a charcoal bed has been set up so that the sensitive parameters, the insensitive parameters, the parameters that need to be measured and the parameters that might usefully be modified to increase the safety of a system can be clearly defined. A simple code has been written which calculates maximum temperatures(or other temperatures) in a bed as a function of time and the pertinent parameters. The code is based on an infinite slab model and should be valuable because it is simple and is quite accurate at higher velocities. A more complicated computer code has also been assembled which is based on a three-dimensional model. This code enables one to mathematically describe a tray-type charcoal adsorber quite accurately, including the heat sink and conduction paths offered by the steel screens and frames. This more detailed thermal analysis is required to estimate temperatures at very low gas flows. Both codes will soon be available.

In the unlikely event of a severe accident with a water or gas-cooled reactor, gaseous fission product iodine may escape the primary containment into the secondary containment. Commonly the plans for coping with this event include charcoal adsorber beds; either in recirculating cleanup systems operating within the secondary containment shell or in a secondary containment exhaust system to a stack.

In the event that these adsorbing beds are used, the decay heat from the collected fission product iodine would tend to heat the charcoal bed. This decay heat plus the fact that charcoal can burn raises two questions: (1) Are there possible conditions which would result in heating the charcoal enough to cause desorption of the iodine and/or ignition of the charcoal? (2) If there are such conditions, can adsorbers be designed and used such that these conditions will always be avoided?

It is only in the most severe accidents that decay heating of charcoal to ignition becomes conceivable. With reference to Fig. 1, it is only the very extraordinary conceived situation with which we are concerned; the situation in which the anticipation and prevention systems within the reactor core have failed, in which the primary containment barrier has

*Research sponsored by the U. S. Atomic Energy Commission under contract with the Union Carbide Corporation.

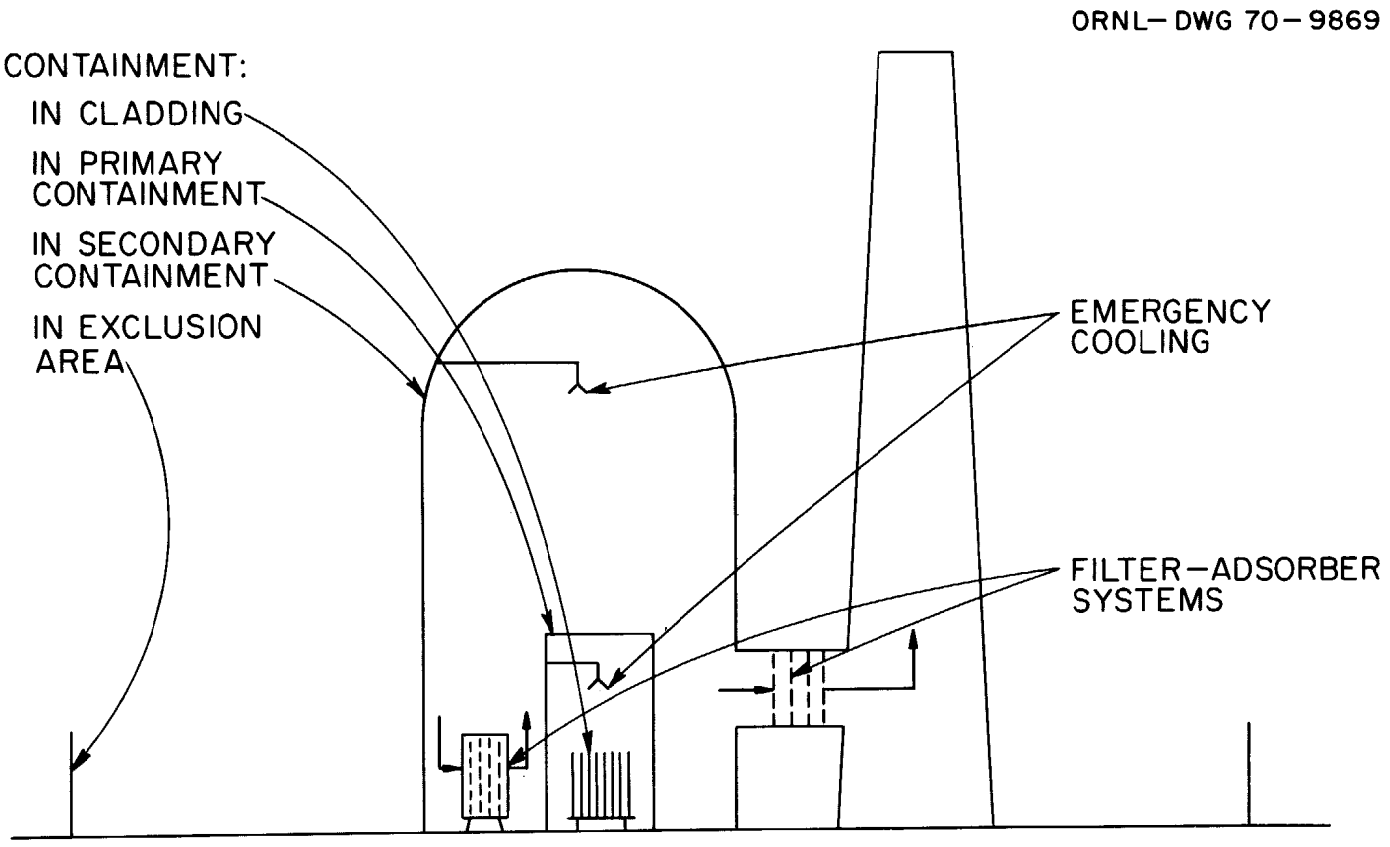

Fig. 1. Some Features of Fission Product Containment Systems.

been breached, in which the emergency core cooling has largely failed and in which the emergency containment cooling has largely failed. In such a case the charcoal adsorbers, either in a recirculating system or in a containment exhaust system, might conceivably become relatively heavily loaded with fission product iodine. If, after all these prior failures, the air moving system also failed so that the air flow through the adsorbers was drastically reduced; the possibility of heatup of the charcoal until iodine desorption and/or ignition took place, is conceivable.

This is clearly an unlikely event but still an important one to consider; the charcoal system is there to ameliorate the hazards of an accident; it must not add to the conflagration.

If the charcoal temperature rises, it will do so because the heat input rate is greater than the heat removal rate. We will consider the heat input first, then the heat balance equation and the other terms in that equation. Figure 2 is a plot of the heat from the decay of the various fission product iodine isotopes and the total decay heat from all the isotopes vs time after shutdown. The units of heat are watts per megawatt of reactor power. Since all the important iodine isotopes have half-lives which are small compared to anticipated fuel life, we presumed that during reactor operation all these isotopes had achieved equilibrium between rates of formation and decay. These equilibrium concentrations in a reactor core depend only on the reactor power level so the decay heat is likewise dependent only on the reactor power, thus $q_{i,o}$ (watts of iodine decay heat from isotope i at zero time after shutdown, per megawatt of reactor power) is approximately:

$$q_{i,o} = E_i Y_i / E_f \qquad (1)$$

($q_{i,o}$ values will be somewhat different than indicated by Eq. (1) due to precursor relations; these have been included in values given later but the details of the relationships will not be discussed here.) $q_{i,o}$ refers to each isotope separately as does E_i, the energy per decay, and the fractional fission yield, Y_i. E_f is the total energy per fission. Also $q_{i,o}$ is made up of beta and gamma energy so one can indicate this as follows:

$$q_{i,o} = q_{i,\beta,o} + q_{i,\gamma,o} = (Y_i/E_f)(E_{i,\beta} + E_{i,\gamma}). \qquad (2)$$

The total energies, $q_{i,o}$ values, for each important isotope[1] as well as the total β, and total γ energy values at reactor shutdown are the indicated zero time points on Fig. 2.

Each isotope decays so the heating rate decreases with time, of course, according to first order kinetics; hence:

$$q_i = q_{i,o} \exp\left(-\frac{0.693}{t_{1/2,i}} t\right) \qquad (3)$$

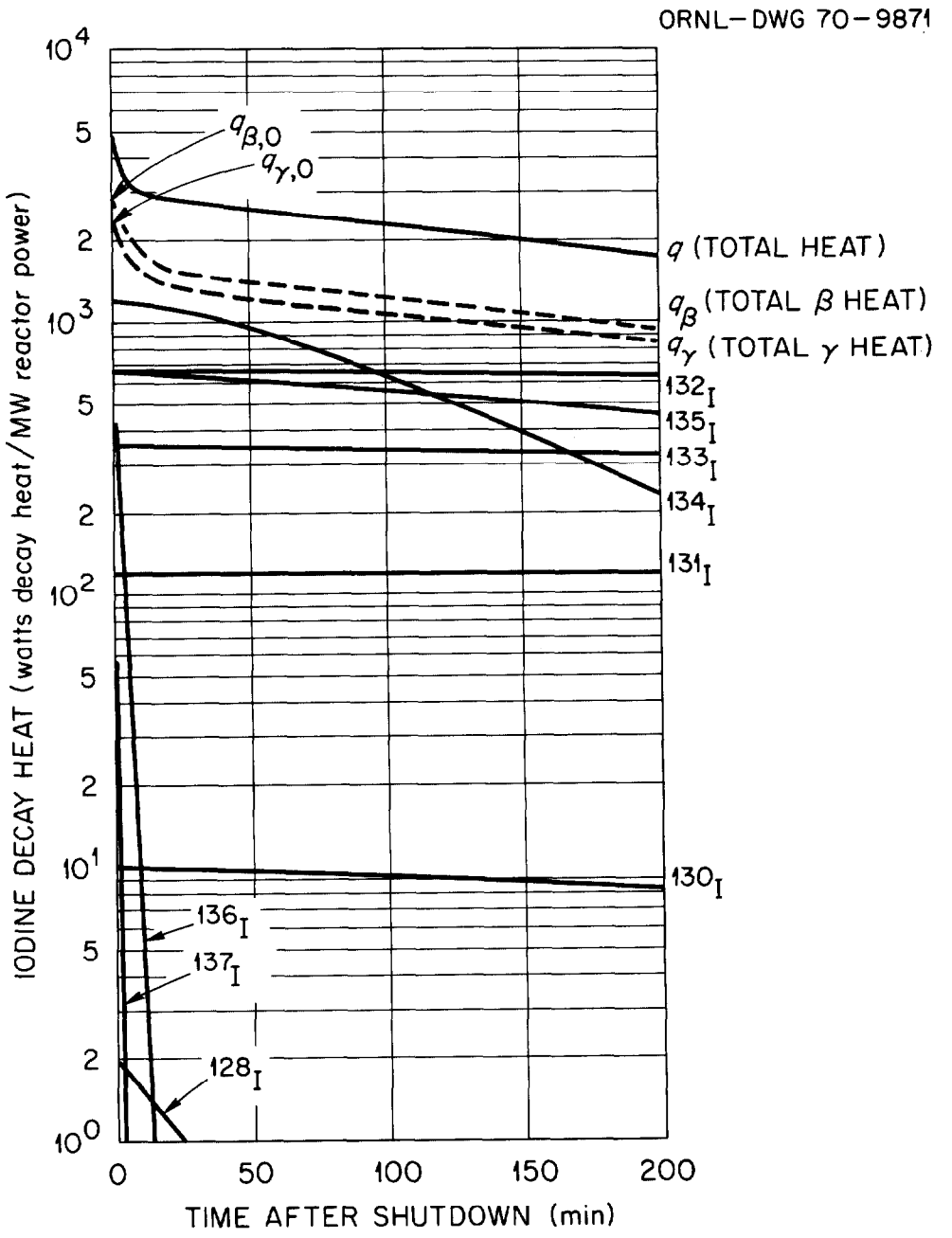

Fig. 2. Fission Product Iodine Decay Heat as a Function of Time after Shutdown.

Some of the q_i values have a more complex time dependence due to precursors; these are also accounted for and explain the non-linearity of some of the q_i vs t times on Fig. 2. Note that the total decay heat of the entire iodine inventory (as seen in Fig. 2) is a few kilowatts per megawatt of reactor power at shutdown; it decreases rapidly in the first 10 minutes after shutdown; it decreases more slowly thereafter.

It is going to be convenient to keep account of these heating rates as the fraction of the total decay energy release rate at shutdown. The ratio of the heating from the β's from all the isotopes, q_β to that at shutdown, $q_{\beta,o}$ is:

$$F_\beta = q_\beta/q_{\beta,o} = \frac{1}{q_{\beta,o}} \sum_i q_{i,\beta,o} \exp\left(-\frac{0.693t}{t_{1/2,i}}\right) \quad (3a)$$

For the γ's:

$$F_\gamma = q_\gamma/q_{\gamma,o} = \frac{1}{q_{\gamma,o}} \sum_i q_{i,\gamma,o} \exp\left(-\frac{0.693\ t}{t_{1/2,i}}\right). \quad (3b)$$

Figure 2 indicates the total iodine decay heat source available; we now will consider various features of a loss-of-coolant accident which will allow us to predict the fraction of this total which can be adsorbed on the charcoal.

First we have accepted 25% as the estimate of the maximum fraction of the iodine which may leave the core. So the fraction released, F_R, is given by:

$$F_R = 0.25. \quad (4)$$

Second, the decrease in decay heat with time, particularly during the first 20 min or so, makes the schedule of iodine release and of iodine loading into the charcoal, of importance. We will consider the three schedules shown in Fig. 3 and their consequences; one will be the conservative assumption that the 25% of the total fission product iodine inventory appears on the charcoal immediately after shutdown. In other words, we presume no fractional holdup due to delay in releasing the iodine; the delay fraction, F_D, is given by:

$$F_D = 1. \quad (5)$$

A second release schedule will be an estimate considering the times required to heat up the core in a loss-of-coolant accident initiated by a sudden double-ended rupture of the main circuit pipe.[2] It has been estimated that for large water-cooled power reactors, the blowdown would consume 5-10 seconds. The cladding might rupture in 30-50 seconds (after fuel heatup to about 1100°C) to allow the so-called prompt release; 10-40% of the iodine inventory may be released from the fuel and it is

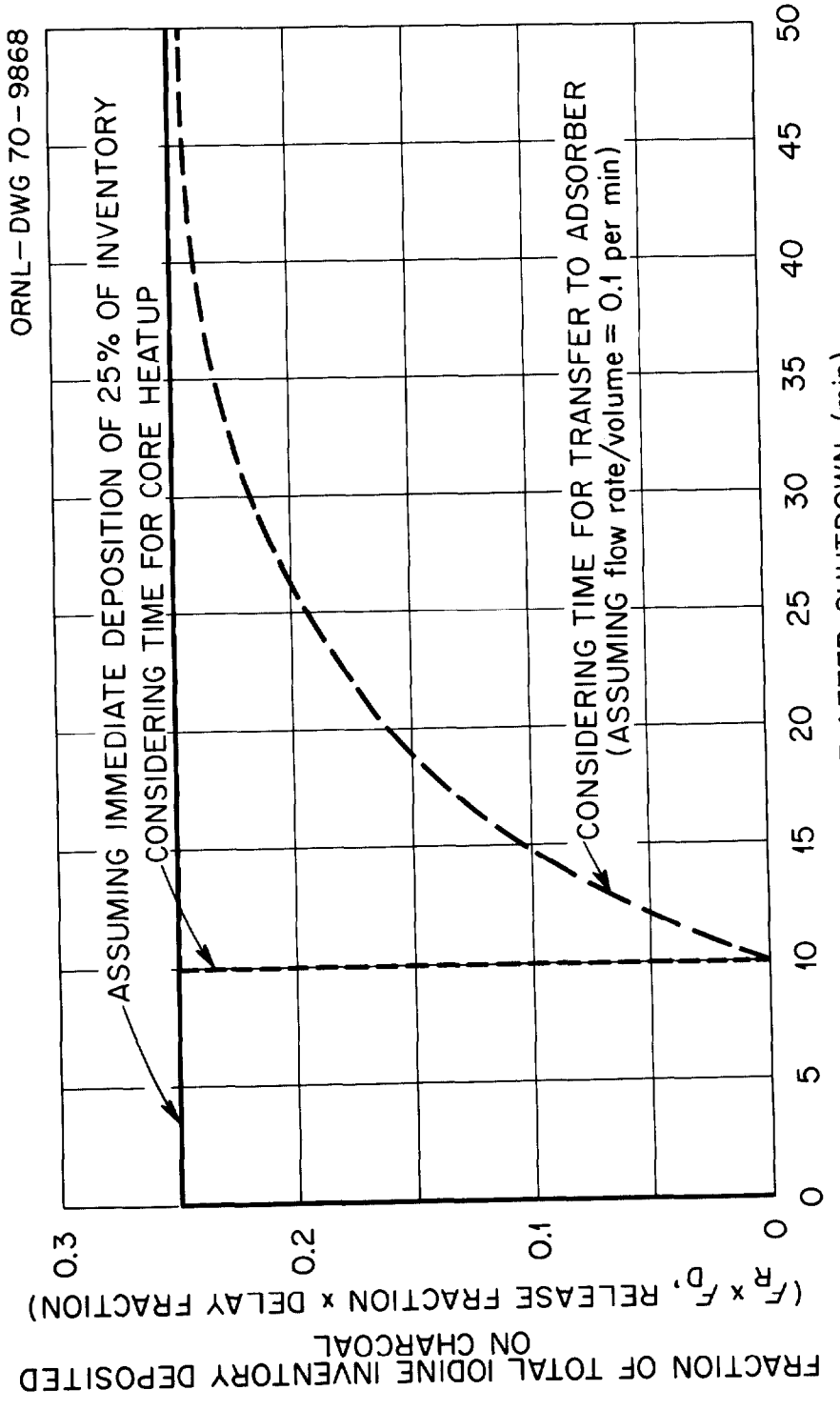

Fig. 3. Possible Schedules of Iodine Deposition onto Charcoal Adsorbers.

estimated that 25% of that might reach the secondary containment. After prompt release, further heating may occur due to decay heat and metal water reactions leading in 10-60 min to fuel melting and release from the fuel of the remainder of the iodine. Presumably, at this time 25% of the total inventory would have been released to the containment.

Since the prompt release is fairly small and since it complicates the calculation, we will assume for the second release schedule, 25% of the inventory to be suddenly adsorbed on the charcoal 10 min after shutdown. In other words, we consider the delay fraction, F_D, to be, from shutdown to 10 min (600 sec) after:

$$F_D = 0 \tag{6}$$

and after 600 sec,

$$F_D = 1. \tag{7}$$

The third schedule also takes into account the time required to transport the iodine from the secondary containment atmosphere to the charcoal. If the iodine is suddenly dispersed into a container of volume V, 10 min after shutdown and then is pumped at a rate R (volume per sec) through the adsorber, the airborne iodine concentration C_a will decrease. In a time increment, dt, C_aRdt units (i.e., g or curies, etc.) of iodine will be deposited (assuming 100% collection efficiency) and the units of iodine in the gas phase will decrease by VdC_a; hence,

$$-VdC_a = C_aRdt \tag{8}$$

$$C_a/C_{a,o} = \exp\left(-\frac{R}{V}[t - 600]\right) \tag{9}$$

where $C_{a,o}$ is a step function; it is 0 from t = 0 to 600 seconds then some value $C_{a,o}$;thereafter $C_a/C_{a,o}$ is the fraction airborne; hence the fraction adsorbed must be $1 - C_a/C_{a,o}$. Therefore, the delay fraction, F_D, for this schedule is (1) from t = 0 to 600 seconds.

$$F_D = 0 \tag{10}$$

and (2) after 600 seconds,

$$F_D = 1 - \exp\left(\frac{R}{V}[t - 600]\right). \tag{11}$$

So thus far we have considered the release fraction, F_R, the fraction of the total inventory which escapes the primary containment, to be 0.25. We have considered the delay fraction, F_D, the fraction of the iodine which escapes the primary and which also has reached the adsorber. We have suggested three illustrative cases of delay fraction; these presume different release schedules which are illustrated in Fig. 3.

We now need to consider the distribution of the heat source on the charcoal bed. We will presume the iodine to have been evenly distributed in terms of the charcoal bed area but to be more concentrated at the front of the bed than the back. We will presume the bed concentration, of adsorbed I_2 decreases exponentially from front to back, according to one equation and the methyl iodide concentration decreases exponentially according to a second equation. We need also to consider separately the gamma and the beta energy; we will presume the beta energy is converted to heat at the site of the radioactive decay, that half of the gamma energy escapes the bed, the other half heats the whole bed uniformly. We will consider the beta energy first.

The iodine (I_2) concentration (g or curies/cm^3 charcoal), B_{I_2} decreases from some concentration, $B_{I_{2,0}}$, at the front of the bed according to:

$$B_{I_2} = B_{I_{2,o}} e^{-b_{I_2} x} \tag{12}$$

where[3]

$$b_{I_2} = 3.65 \text{ per cm} \tag{13}$$

The methyl iodide concentration is presumed to decrease according to:

$$B_{MeI} = B_{MeI,o} e^{-b_{MeI} x} \tag{14}$$

with[3]

$$b_{MeI} = 0.40 \text{ per cm} \tag{15}$$

We will presume that the fraction of iodine existing as I_2, F_{I_2} to be:

$$F_{I_2} = 0.9 \tag{16}$$

and the fraction as methyl iodide,

$$F_{MeI} = 0.1 \tag{17}$$

The average concentration of I_2 in the bed, $B_{I_2,avg}$, is F_{I_2} times the total iodine loading, L (g or curies etc. per sq cm of bed) divided by the thickness of the bed, S; hence:

$$B_{I_2,avg} = F_{I_2} L/S \tag{18}$$

But the total I_2 loading ($F_{I_2} L$) is the integral of the I_2 concentration over the bed thickness, hence:

$$B_{I_2,avg} = 1/S \int_0^S Bdx = [B_{I_2,o}/S] \int_0^S e^{-b_{I_2}x}$$

$$B_{I_2,avg} = [B_{I_2,o}/Sb_{I_2}](1 - e^{-b_{I_2}S})$$

and

$$B_{o,I_2} = Sb_{I_2} B_{I_2,avg}/(1 - e^{-b_{I_2}S}) \quad (19)$$

On combining with Eq. (18):

$$B_{o,I_2} = b_{I_2} F_{I_2} L/(1 - e^{-b_{I_2}S}). \quad (20)$$

Combining with (12) gives:

$$B_{I_2} = [b_{I_2} F_{I_2} L/(1 - e^{-b_{I_2}S})]e^{-b_{I_2}x} \quad (21)$$

So the fractional concentration at x, i.e., the ratio of the concentration B_{I_2} at x to the average concentration L/S, is:

$$F_{I_2,x} = B_{I_2} S/L = F_{I_2} b_{I_2} S[e^{-b_{I_2}x}/(1 - e^{-b_{I_2}S})] \quad (22)$$

Similarly, for methyl iodide:

$$F_{MeI,x} = B_{MeI} S/L = F_{MeI} b_{MeI} S[e^{-b_{MeI}x}/(1 - e^{-b_{MeI}S})] \quad (23)$$

The sum of these fractions, F_x, is

$$F_x = F_{I_2,x} + F_{MeI,x} \quad (23a)$$

These fractions, $F_{I_2,x}$, $F_{MeI,x}$, and the sum of the two are plotted vs bed depth for a 5 cm (2") bed on Fig. 4.

So the rate of beta energy released (watts of decay heat/Mw of reactor power) will be the total beta heating rate of the iodine inventory at shutdown; $q_{\beta,o}$, multiplied by the sequence of fractions which have been developed. Hence:

$$q_\beta = q_{\beta,o} (F_R F_D F_x F_\beta) \quad (24)$$

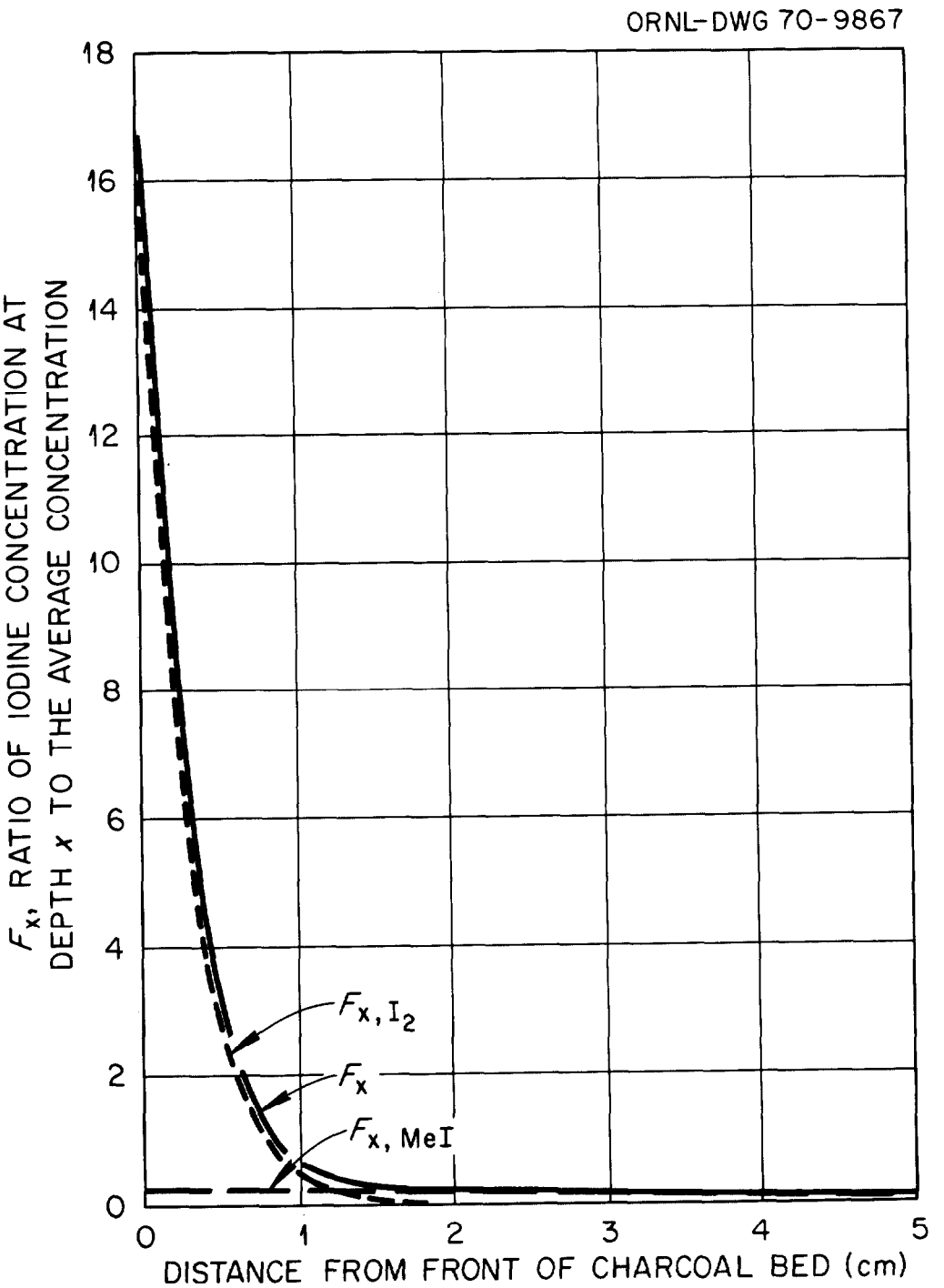

Fig. 4. Iodine Loading vs Depth in the Charcoal Bed.

It is convenient also to consider a $q_{\beta,avg}$, the β heating value at the position in the bed where the iodine concentration is the average value, i.e., where F_x is unity, hence:

$$q_{\beta,\ avg} = q_{\beta,o}\ (F_R F_D F_\beta) \tag{24a}$$

For the gamma heating, we presume no bed depth (x) dependence; also it is presumed that a fraction, F'_γ of the gamma heat escapes the bed. We presumed:

$$F'_\gamma = 0.5 \tag{25}$$

Hence the gamma heating rate is

$$q_\gamma = q_{\gamma,o}\ (F_R F_D F'_\gamma F_\gamma) \tag{26}$$

Of course, the total heating rate is:

$$q = q_\beta + q_\gamma \tag{27}$$

and at the bed position where the iodine concentration is the average value,

$$q_{avg} = q_{\beta,avg} + q_\gamma \tag{27a}$$

The values of parameters (in some cases per MWt of reactor power) are given in Figs. 2-4. Figure 5 is a plot of q_{avg} vs time for the three charcoal bed loading schedules described earlier (and on Fig. 3).

We wish eventually to know the heating in terms of watts per cm^3 of charcoal bed. If we define q''' as this heating term (watts/cm^3), then:

$$q''' = q\ \frac{P}{AS} \tag{27b}$$

and at the bed position where the average iodine concentration exists,

$$q'''_{avg} = q_{avg}\ P/AS \tag{27c}$$

where P is the reactor power (Mwt). A is the area of the charcoal bed and S is the thickness. Figure 5 also shows example values of q'''_{avg} as a function of time based on a P/AS ratio of 0.25×10^{-3} Mwt/cm^3.

A computer code has been written[4] which calculates q'''; it outputs the maximum values of q''' for the front of the bed (where F_x in Fig. 4 and Eq. (24) is a maximum), the minimum value of q''' at the rear of the bed (where F_x is a minimum) and the average value of q''' where F_x is unity. As might have been anticipated, with the assumption of no delay between reactor shutdown and adsorption on the bed, the calculated heat loads are initially high. With the inclusion of the time delays the maximum, average heat load is considerably reduced.

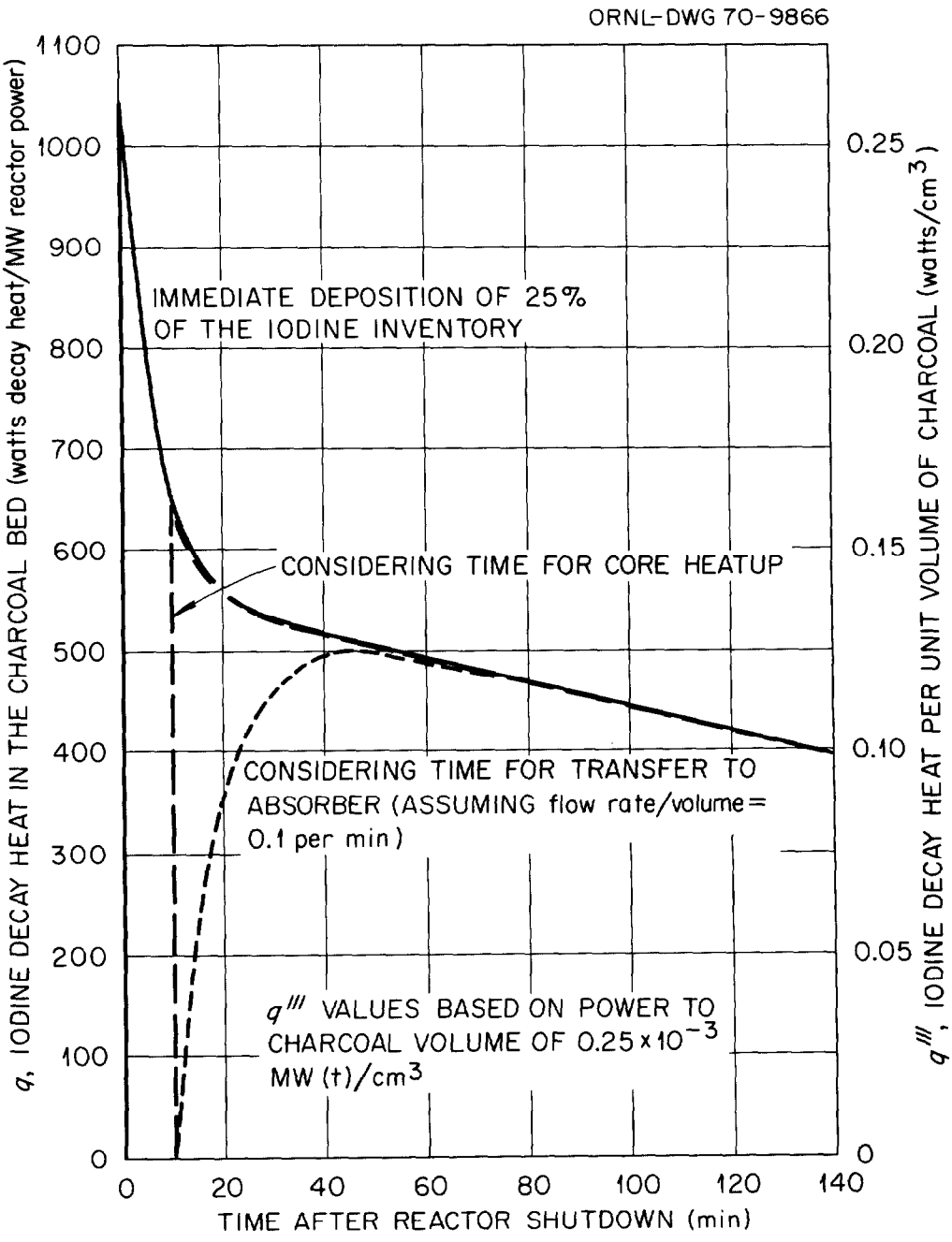

Fig. 5. Heat Source in Charcoal Beds.

We have now evaluated the heat generation term of an equation expressing the heat balance in a charcoal adsorber bed. We need now to consider the rest of the equation. This has been done at two levels of sophistication, represented by two models of an adsorber bed. First, we will consider an infinite slab model. In this model a bed of thickness S of charcoal granules is considered, heat is presumed only to flow in the thickness (x) direction (as if the bed were of infinite length and width). The steel plates which contain the charcoal are not considered, either as a heat sink or conduction path. The heat balance equation for any point in the bed is

$$\rho_b C_{p_b} \frac{\partial T_b}{\partial t} = K_b \frac{\partial^2 T_b}{\partial x^2} + q''' - H(T_b - T_g). \tag{28}$$

The first term expresses the heat absorbed in the charcoal granules; the density ρ_b (g/cm^3) times the heat capacity C_{p_b} (watt-sec/g-°C) times the rate of temperature rise $\partial T_b/\partial t$ (°C/sec). The units of the whole term are watts/cm3. The second term expresses the heat conducted to the point for which the heat balance pertains; hence K_b is the thermal conductivity of the bed (watt/cm2(°C/cm)), $\partial^2 T_b/\partial x^2$ is the change in the temperature gradient with x (°C/cm^2). The third term is the heat generation term developed above and summarized in Eq. (24, 26, and 27). The fourth term expresses the heat removal by the flowing air. H is called the volumetric heat transfer coefficient (watt/cm^3 °C); T_b and T_g are respectively the charcoal bed and the gas temperatures.

One needs values of bed density, ρ_b, bed heat capacity, C_{p_b}, bed thermal conductivity, K_b, and the bed volumetric heat transfer coefficient H. We are in the process of experimentally determining these parameters; for this report we will use the following values:

$$\rho_b = 0.56 \text{ g/cm3} \tag{29}$$

$$K_b = 0.124 \text{ watts/cm}^2(°C/cm) \tag{30}$$

$$C_{p_b} = 0.47 \text{ watt sec/g-°C} \tag{31}$$

$$H = 0.022\, V_g^{0.66} \text{ watts/cm}^3\text{-°C} \tag{32}$$

where V_g is the air velocity (cm/sec) through the adsorber. The value of H, the volumetric heat transfer coefficient was estimated on the basis of correlation of heat transfer measurements in packed beds.[5]

The infinite slab model is most applicable at reasonably high gas flows and under this condition the gas temperature does not rise much so can be considered constant. If we define T_b' as

$$T_b' = T_b - T_g \tag{33}$$

and T_g is a constant, then Eq. (28) becomes

$$\rho_b C_{p_b} \frac{\partial T_b'}{\partial t} = K_b \frac{\partial^2 T_b'}{\partial x^2} + q''' - HT_b' \qquad (34)$$

By means of a change of variable, Eq. (34) was solved analytically.[4] A computer code has been written of this solution which outputs temperature values at desired locations in the bed, maximum temperatures or a plot of maximum temperature vs time. A code has also been written which provides a numerical solution; a general heat transfer code, HEATING2 was used for the purpose. The numerical solution code is more versatile in that it readily accepts parameters (K_b, H, C_{p_b}) as functions of time and temperature. The two calculations have been shown to give the same answer for test cases.

Figure 6 shows maximum bed temperatures vs time for two air velocities, and for the loading schedule indicated by equations (6) and (7), (i.e. for sudden iodine loading onto the bed 10 minutes after shutdown). The times on this plot refer to time after the iodine loading has started, in other words these time values are 10 minutes less than time after shutdown. It is noted that an air velocity of 40 ft/min is a common design value.

Figure 7 is a similar plot of maximum temperatures vs time for several air velocities and for the loading schedule indicated by equations (10) and (11), (with R/V, i.e. the air flow rate over the containment volume, of about 0.1 per minute). The times on this plot also refer to time after iodine loading has started (or time after shutdown minus 10 minutes).

These two figures (i.e. 6 and 7) demonstrate that the air velocity and the schedule of iodine loading are very important parameters. This infers that the most hazardous situation might be one in which loading of the iodine occurred quickly and in which a low flow condition developed soon after loading. Figure 8 indicates how the maximum temperature in the charcoal beds might change in that situation. Specifically the Fig. 8 temperatures were calculated assuming a normal flow (40 ft/min) for long enough to load 95% of the iodine which would eventually be loaded and assuming a low flow (4 ft/min) after that. As can be seen, the maximum temperature in this case was modest (in comparison to ignition temperatures which are commonly over 600°F).

Finally, we need to consider the three-dimensional model which not only considers the charcoal granules and heat transfer in the x direction but also the steel screens and frames and heat transfer in the y and z directions. The general heat balance equation for any point in the system is:

$$\rho_i C_i \frac{\partial T_b}{\partial t} = K_i \nabla^2 T_b + q''' - H(T_b - T_g). \qquad (35)$$

ORNL-DWG 70-10506

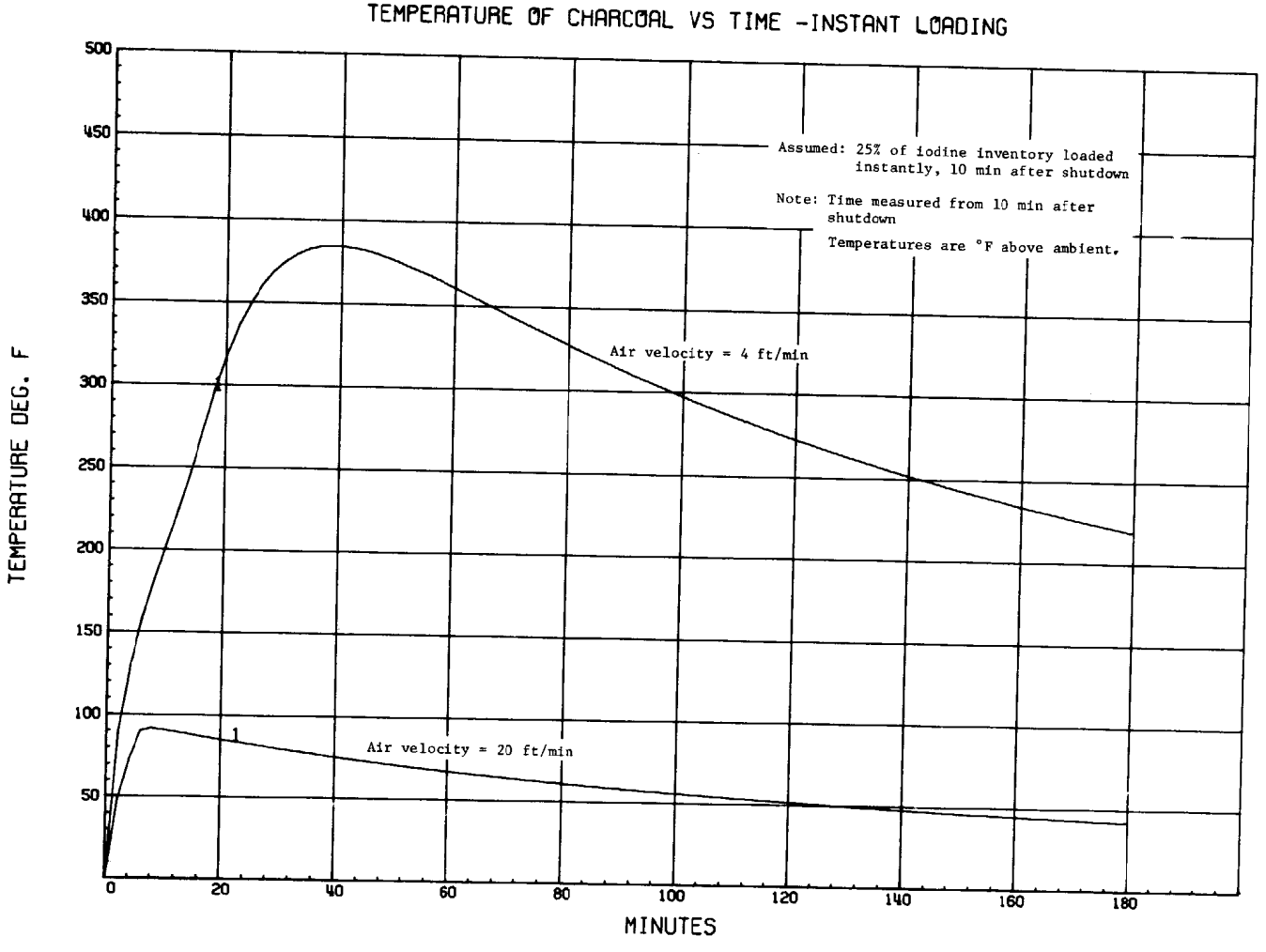

Fig. 6. Maximum Charcoal Temperature vs Time for Instant Loading 10 Minutes After Shutdown

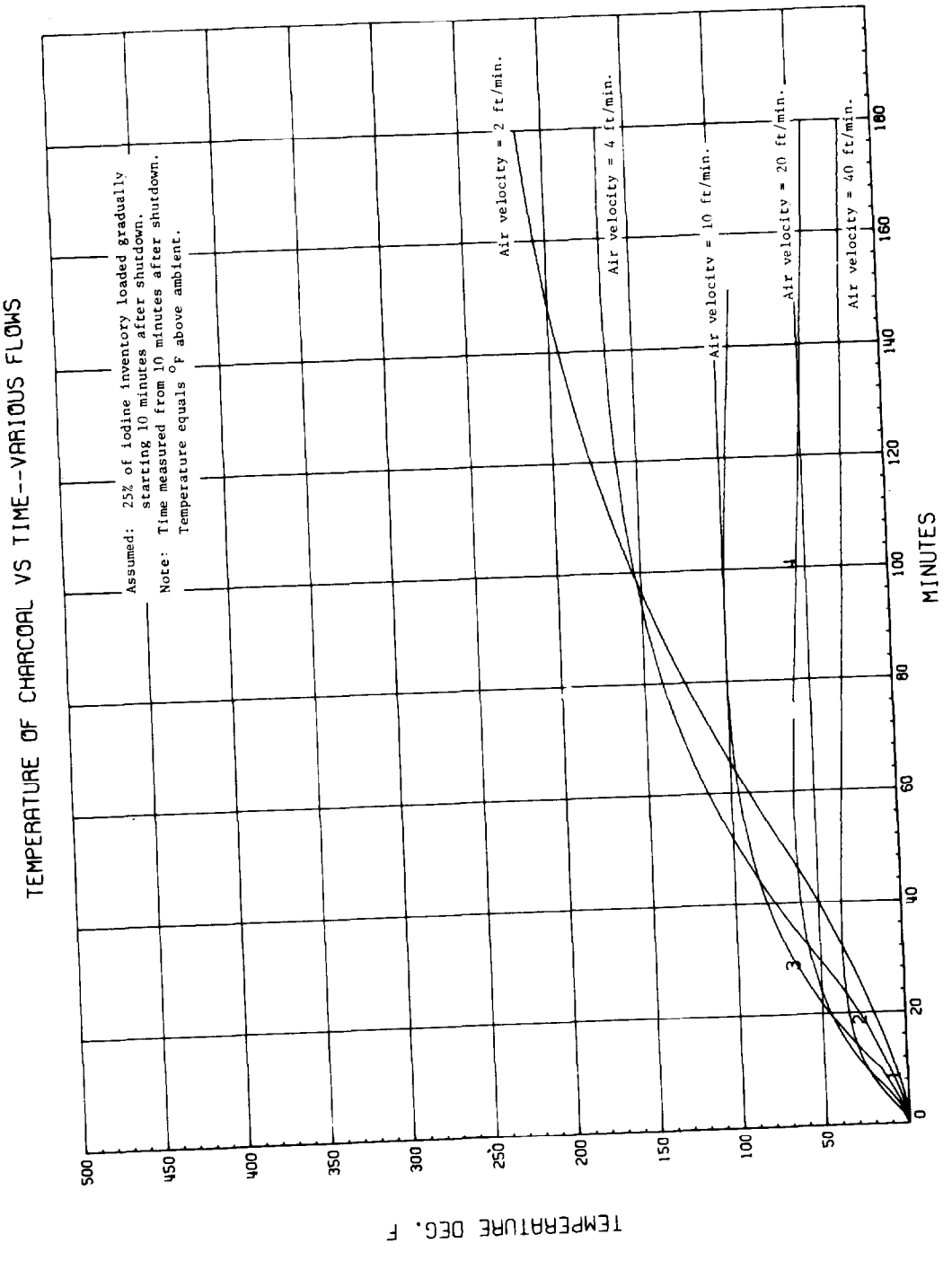

Fig. 7. Maximum Charcoal Temperature vs Time for Gradual Loading

ORNL-DWG 70-10507

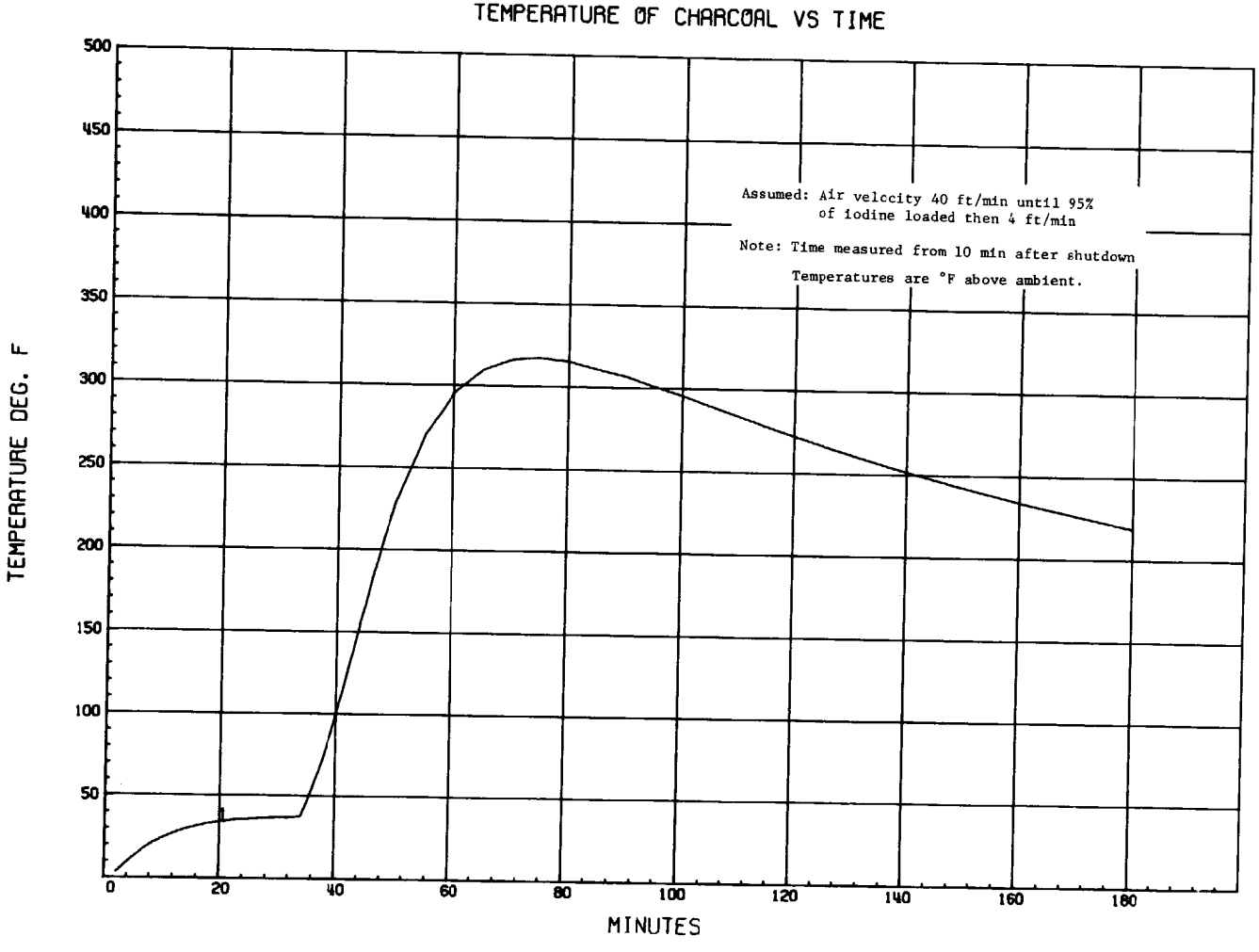

Fig. 8. Maximum Charcoal Temperature vs Time for High Air Flow Followed By Low Air Flow

This equation appears similar to Eq. (28); except the $K_i \nabla^2 T_b$ term considers heat conduction in three directions and as indicated by $\rho_i C_i$ and K_i, we consider all the materials present in the absorbers as heat sinks and as conduction paths. Equation (35) is not analytically soluble; a general heat transfer computer code, HEATING2[4] was modified for the purpose and is called HEATING3.[4] It is a general transient three-dimensional code written in FORTRAN IV for the IBM 360. It accepts rectangular or cylindrical geometry; it can handle 2000 lattice points, 100 regions, 50 materials and 50 boundary conditions. The boundary conditions may be non-linear (like natural convection or radiation heat transfer) or linear (like force convection heat transfer). It can handle problems with heat transfer from surface to surface (like in radiation from one slab to another). The heat generation in each region can be a function of position and/or time.

Figure 9 is a drawing of a particular geometry (i.e., charcoal bed and steel frame dimensions) for which some calculations have been made. On this drawing the steel frame is indicated accurately and so are some of the details of accurately locating, with Cartesian coordinates, the positions of the steel frame. The locations of the charcoal beds sandwiched between steel screens are approximately indicated with dashed lines. The direction of air flow through the system is also indicated. This geometry is similar to that of the tray-type adsorber unit as shown in Fig. 10.

In summary, the problem of estimating maximum temperatures in a charcoal bed has been set up so that the sensitive parameters, the insensitive parameters, the parameters that need to be measured and the parameters that might usefully be modified to increase the safety of a system can be clearly defined. A simple code has been written which calculates maximum temperatures (or other temperatures) in a bed as a function of time and the pertinent parameters. The code is based on an infinite slab model and should be valuable because it is simple and is quite accurate at higher velocities. A more complicated computer code has also been assembled which is based on a three-dimensional model. This code enables one to mathematically describe a tray-type charcoal adsorber quite accurately, including the heat sink and conduction paths offered by the steel screens and frames. This more detailed thermal analysis is required to estimate temperatures at very low gas flows. Both codes will soon be available.

ORNL-DWG 70-10025R

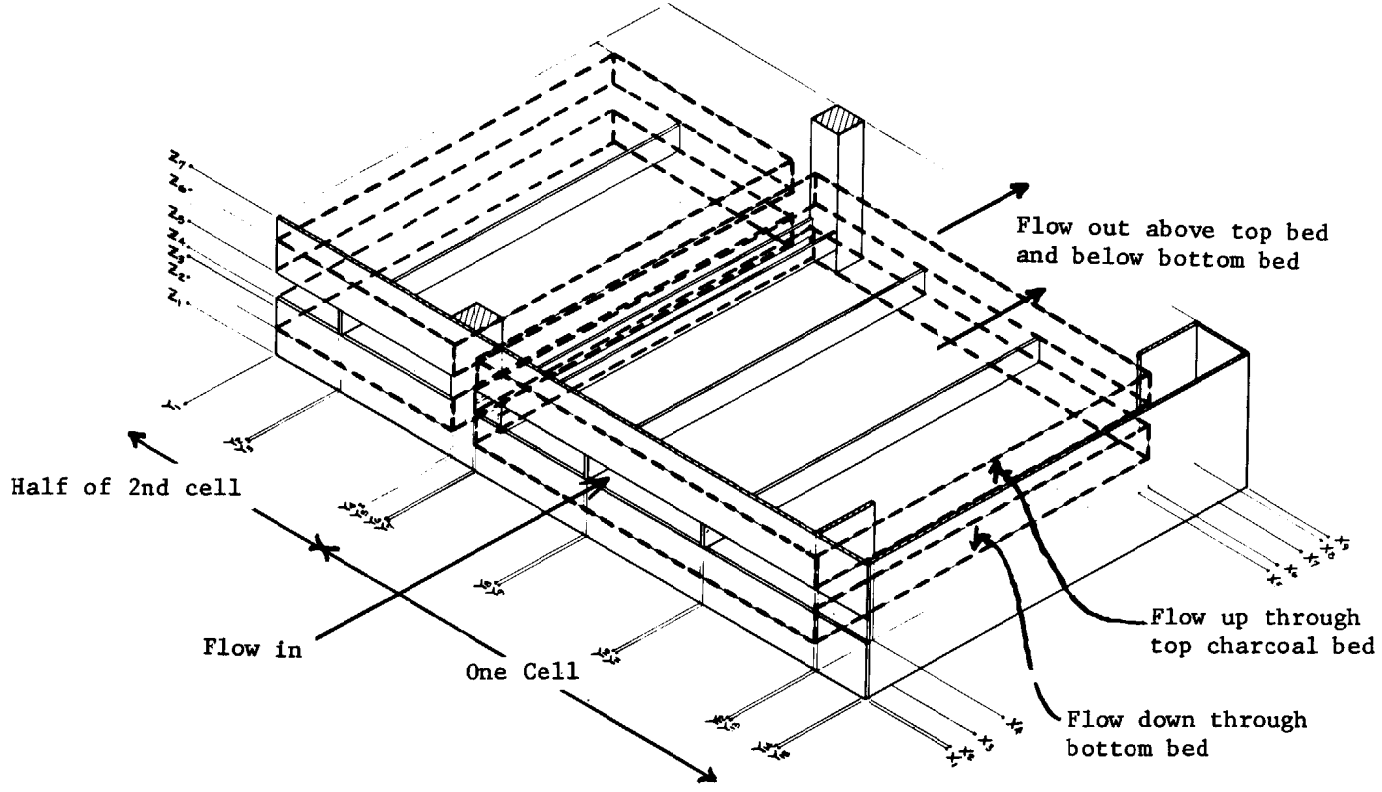

Fig. 9 Three Dimensional Model

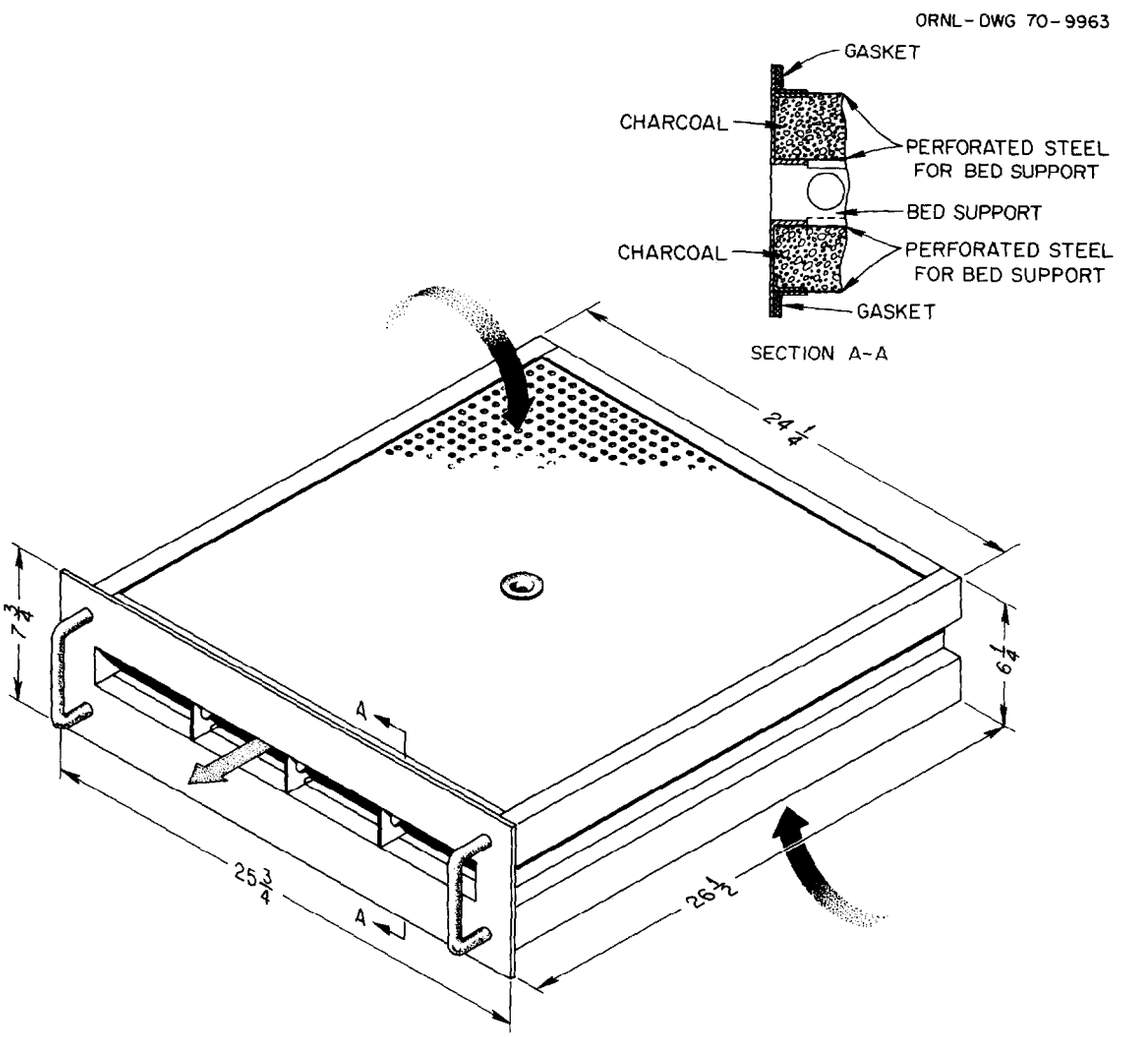

Fig. 10. Tray-Type Charcoal Adsorber

References

1. M. J. Bell, Chemical Technology Division Annual Progress Report for the Period Ending May 31, 1969, ORNL-4422, pp. 89-94.

2. Advisory Task Force on Power Reactor Emergency Cooling, W. K. Ergen, Chairman, "Emergency Core Cooling," USAEC Report.

3. R. D. Ackley, Reactor Chemistry Division, Oak Ridge National Laboratory, private communication.

4. R. P. Shields and M. Siman-Tov, "The Effect of Iodine Decay Heat on Charcoal Adsorbers," ORNL-4602, report in preparation.

5. J. E. Coppage, Ph.D. Thesis, Mechanical Engineering Department, Stanford University, 1952.

R. J. Davis presented Mr. Shields' paper.

DISCUSSION

KOVACH: Does the atmospheric composition resemble what we can expect in an incident when you would adsorb with say decay heat?

DAVIS: Is your question with reference to the amount of iodine?

KOVACH: No, I'm talking about steam or what ever else you may have present in the atmosphere under these conditions.

DAVIS: I don't think that there was anything in the calculations that depended on steam concentration.

KOVACH: Can we use the equation actually to calculate what may happen in an actual incident to the carbon as far as the heat is concerned?

DAVIS: That's what we are suggesting, yes. We have stated assumptions and made calculations on that basis. One can readily use the code to estimate temperatures based on other assumptions. You mentioned steam, when you first bring water into a dry charcoal bed, it will heat up. But we don't think that this should seriously matter because the steam and its heat effect will be over with before the iodine arrives.

NEW FIRE PROTECTION SYSTEMS FOR FILTER PLENUMS

W. E. Domning

The Dow Chemical Company
Rocky Flats Division
P. O. Box 888
Golden, Colorado 80401

ABSTRACT

A fire test facility has been constructed at Dow, Rocky Flats consisting of a glovebox and a filter plenum which contained 12 filters. The purpose of this facility is to study the effects of a fire originating within the glovebox on the entire glovebox system which includes the filter plenum. The details of construction of the facility are shown and the results of several experiments are discussed to show the capability of the facility.

Exhaust air temperatures from burning shielded gloveboxes range between 1530 to 1620°F. In order to maintain filter integrity under these conditions it is necessary to cool the air stream prior to filtration. The most successful air cooler tested has been a water spray-cooled baffle inserted upstream of the initial stage of filtration. This baffle was effective in cooling 1672°F incoming air to 125°F within one minute after actuation.

Introduction

The fire which occurred in Building 776 at Rocky Flats on May 11, 1969 has prompted investigation of a glovebox system under fire conditions. The glovebox system that existed in Building 776 at the time of the fire was a series of gloveboxes connected by conveyor lines. The conveyor boxes were used as air exhaust plenums from the gloveboxes with dry air entering the boxes. The conveyor line was exhausted by two 4-stage HEPA filter plenums and fan units. The windows of the gloveboxes were primarily of Plexiglas SE-3®. Glove rings were mounted in the window areas. Shielding comprised of Benelex® and Plexiglas G® had been added to the

exterior of the gloveboxes and the conveyor line. This shielding varied between 2 and 4 inches in thickness and for the most part covered the bottom and sides of the boxes and conveyor lines.

The fire spread through the entire conveyor system, plugging the filters of one plenum system and burning out the Plexiglas windows of the conveyor and some gloveboxes until it reached the second exhaust plenum. Several stages of filtration were breached in this plenum by the high temperature air generated by the fire.

The magnitude of the fire, its rate of spread, and the difficulties encountered in extinguishing it were initial questions. Later it became evident that a reevaluation of fire protection for HEPA filters should be undertaken.

In order to develop and test new methods for fire protection, a fire test facility has been constructed at Dow, Rocky Flats. This facility consists of a glovebox, controls, and instrumentation.

Considerable work has been conducted in the past on glovebox fires; however, the scope of the work has been limited to the glovebox and its contents, and the work can essentially be divided into two categories; evaluation of materials and evaluation of extinguishers. In previous work reported, the experiments considered neither the effects of air flow nor the effect of a fire on the protective filter system.

It is very important that the glovebox and filter be considered as a single system for fire protection. Figure 1 shows the interrelation of the components that make up a typical glovebox facility. A filter plenum and its filters should not be damaged as a result of fire fighting efforts, therefore the filters should not be exposed to either high temperature air or to water. It is apparent that plugging of the building exhaust filters from smoke would cause a loss of negative pressure within the building, and consequent spread of radioactive contamination. However, if the filters in the system serving the glovebox should plug, the results would not be serious since containment would still be effected by the surrounding building.

The fire test facility at Dow, Rocky Flats has been designed to study the interaction between the glovebox and

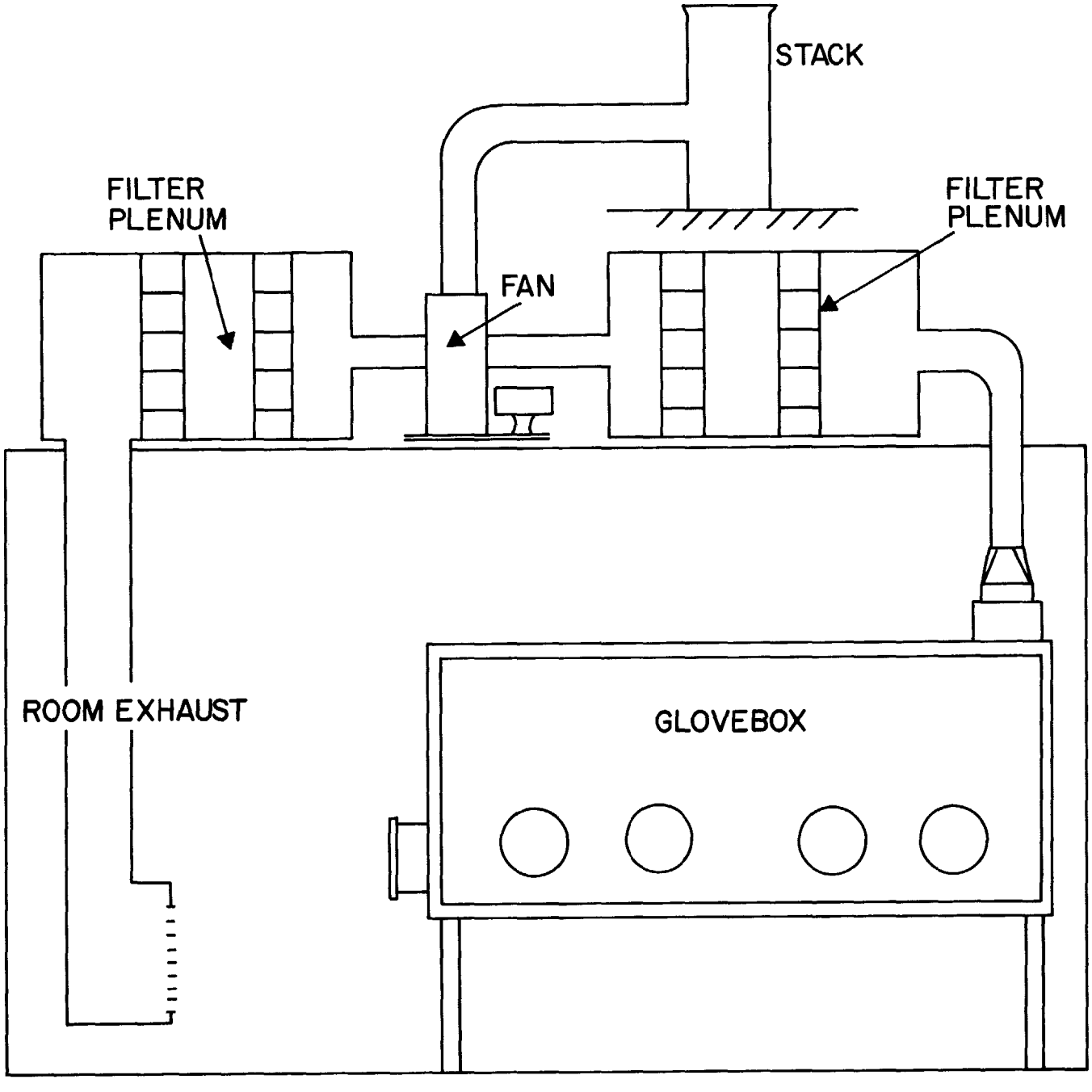

Figure 1 Glovebox System

the filter plenum as well as provide the designer and fire protection engineer with sufficient data to prove the fire safety of an installation.

Description of Facility

Figure 2 shows a general view of the facility. A test glovebox, which can be shielded, is shown at the left of Figure 2, and Figures 3 and 4 illustrate the glovebox shielding configuration. The taller building is the burning test building and is constructed to simulate a"typical room" condition for a glovebox. The ceiling of the building is 12 feet high and the walls of the building, which act as heat reflectors, are approximately 4 feet from the exterior of the glovebox. The building on the right of Figure 2 is the test filter plenum. A fan, with a maximum capacity 10,500 CFM, is connected to the filter plenum.

To the rear of the burning building is a small instrument house. Three recorders provide 14 points of thermocouple readout. Pressure sensing instrumentation and electrical controls are also located nearby.

Figure 5 is a view of the filter plenum under construction. The inlet end of the plenum is a steel bulkhead to withstand the high temperature of the incoming air. The remainder of the plenum is covered with asbestos-cement board. All joints are battened and caulked to provide a leakproof structure. The floor of the plenum is made from road-mix gravel and is built-up about 1 foot from the ground-level to allow for water drainage.

A water spray-cooled baffle forms the inlet section of the plenum and two filter-holding frames divide the plenum into three additional sections. A window and access door is installed in each section. High intensity flood lamps are mounted in the ceiling of the plenum to aid test viewing.

Figure 6 shows the partially completed water spray-cooled baffle. The baffle is made from 6-inch, 10.5 lb/ft channel iron members. The channels are staggered to form a tortuous path for the air. One of the two channel support members is movable and adjustment screws are provided to vary the distance between the toes of the channels. The present setting is such that the open area between the channels is equal to the filter face area. Figure 7, a close-up of the baffle construction, shows the adjustable space between the two portions of the baffle.

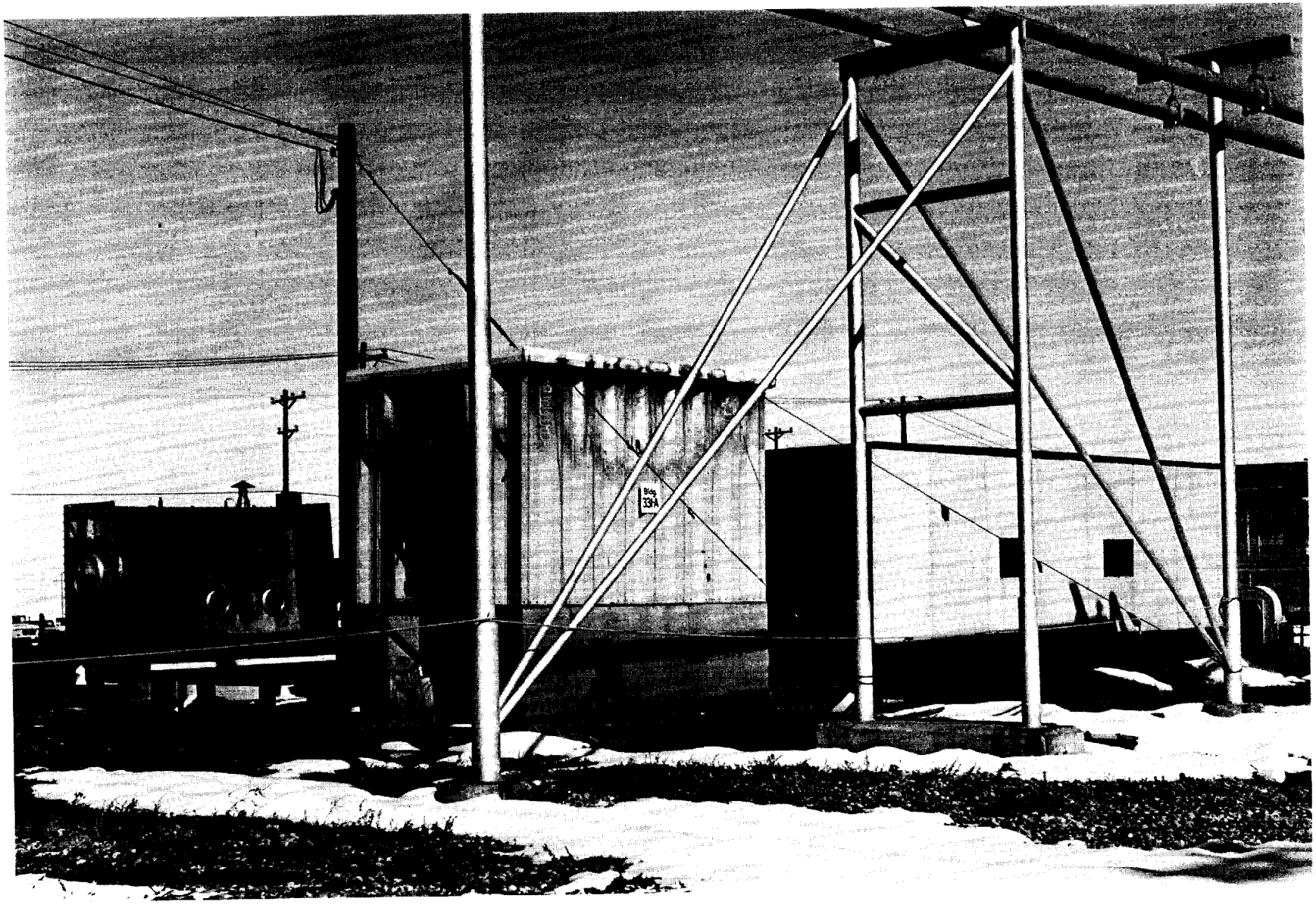

FIGURE 2

Fire Test Facility

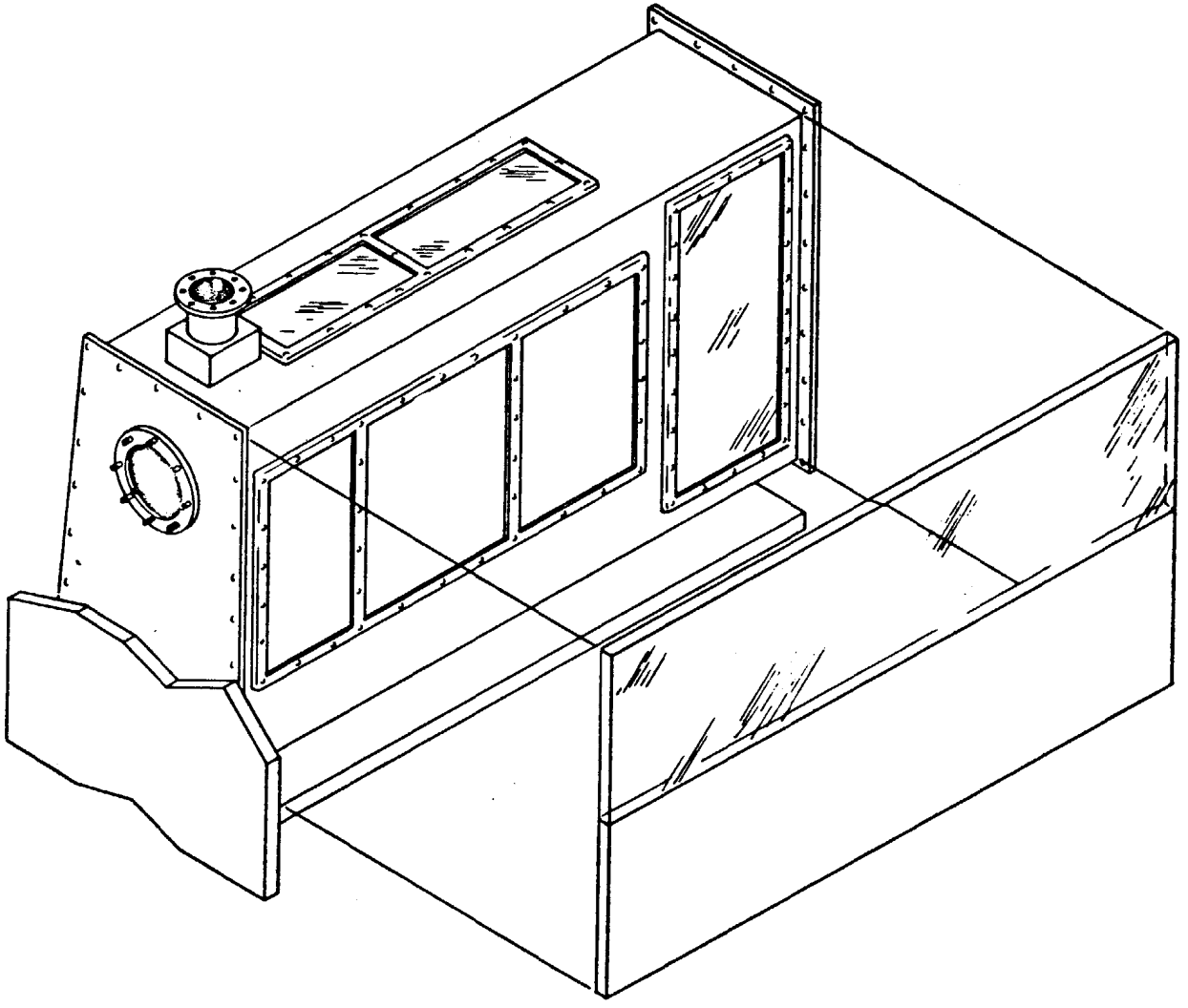

FIGURE 3
Glovebox and Shielding
Arrangement - Straight Side

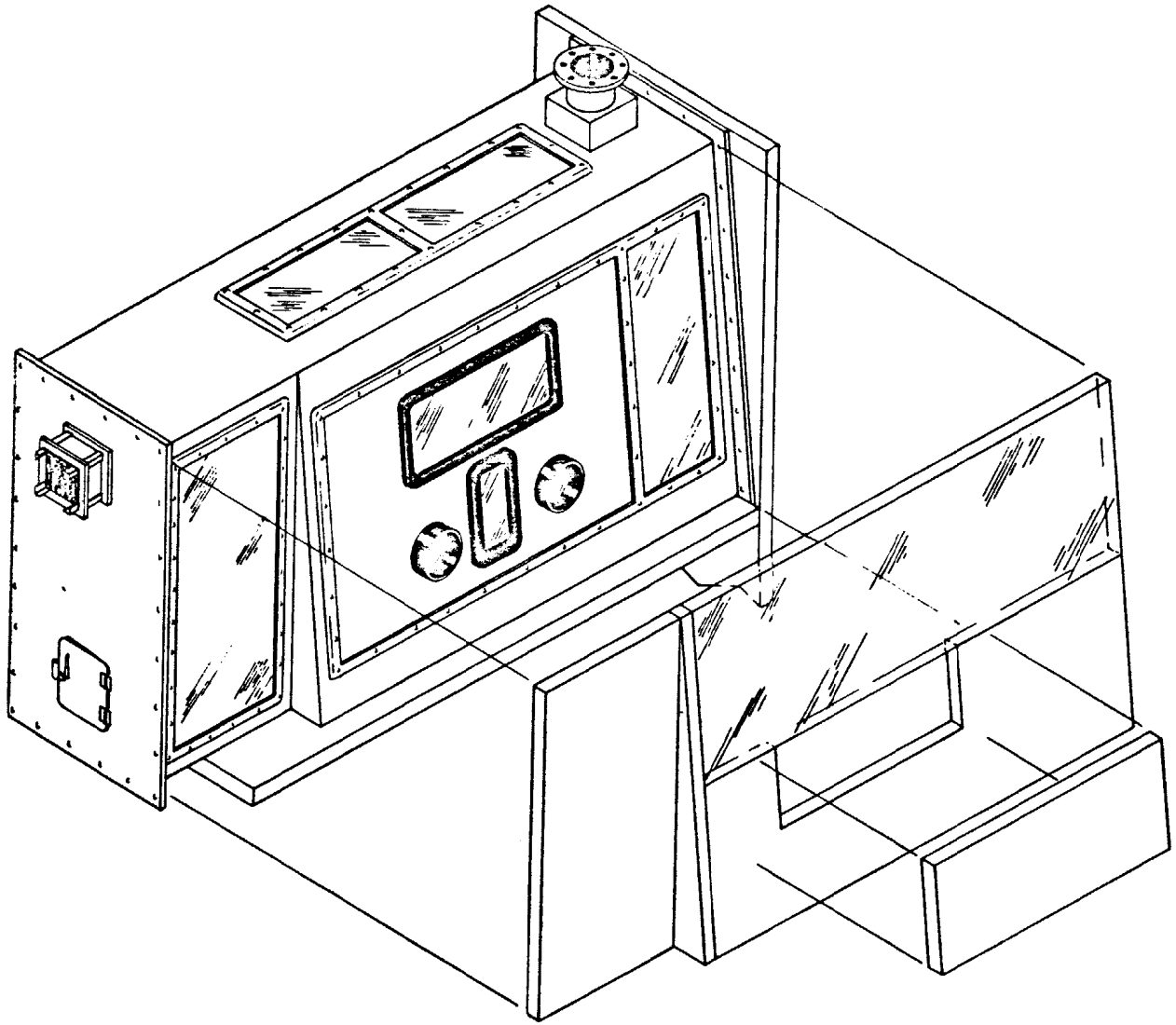

FIGURE 4
Glovebox and Shielding
Configuration - Sloped Side

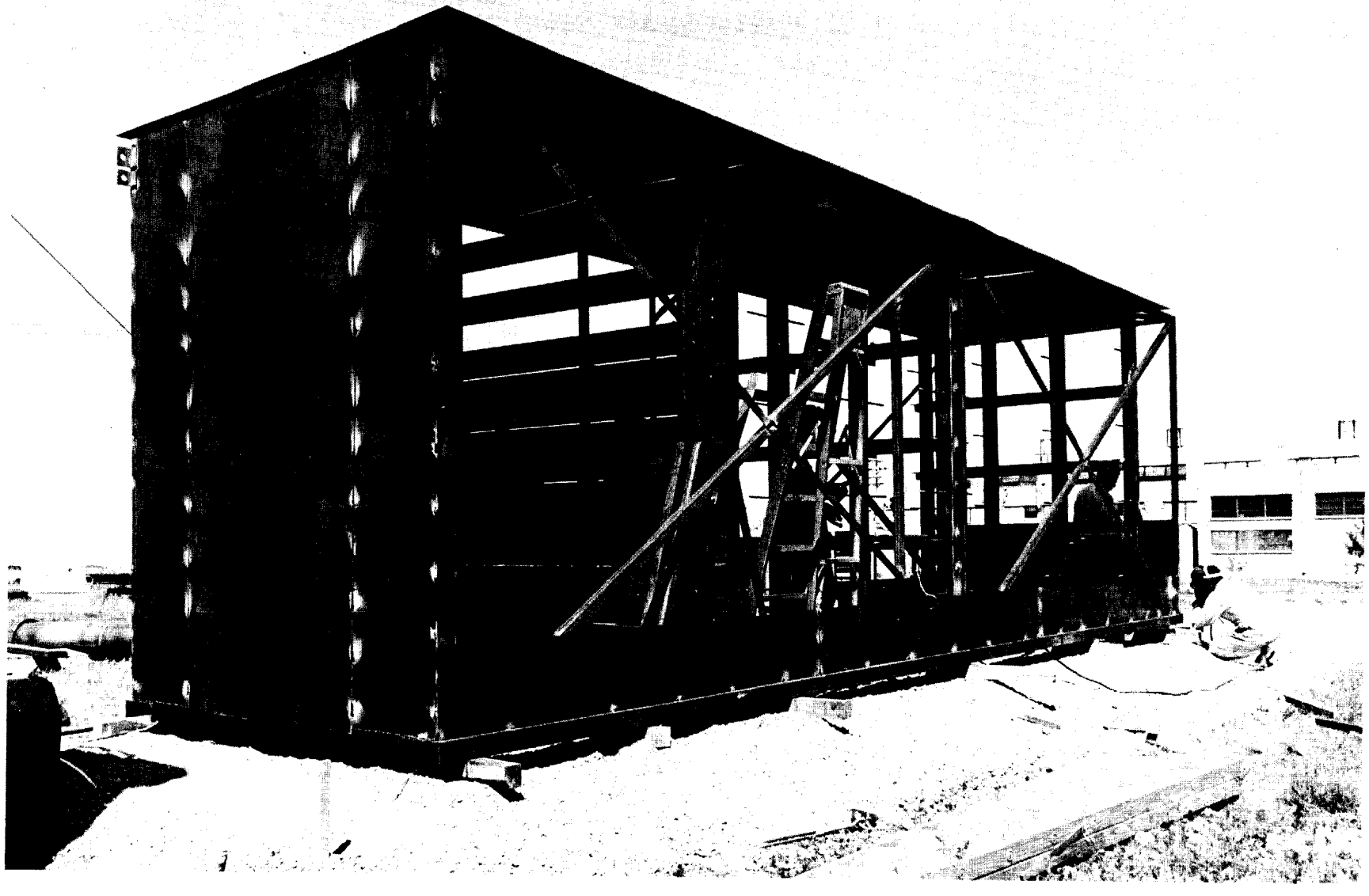

FIGURE 5

Filter plenum
under construction

FIGURE 6

Partially finished baffle

FIGURE 7

Detail of baffle construction

The channel members are easily removed so than an inlet pipe may be added to by-pass the baffle, and simulate existing plenum construction. Figure 8 shows the relationship between the upstream and downstream filter frames. Twelve 2 feet by 2 feet by 1 foot HEPA filters are installed in each frame.

The construction details of the filter-holding frame are shown in Figure 9. The upright members are made from 3 inch by 5 inch square structural tubing (CRS). The cross members are made from 3 inch by 4 inch square structural tubing (CRS). Hold-down studs are fabricated from 5/8-inch 304 stainless steel rod. Filter supports are fabricated from 3 inch by 4 inch structural tee members. Hold-down bars, compressed by nuts on the stud furnish the pressure necessary to seal the filter to the frame.

A 2-inch header pipe and valving is piped into each section for water supply. Additional branch piping is available for spray or sprinkler heads as desired. A water-flow meter and pressure gauges are available for calibration of nozzles.

Discussion of Experiments Performed

Two experiments have been performed relative to fire suppression in burning gloveboxes. Unfortunately, these experiments were performed before the filter plenum was constructed; therefore, experiments concerned with the interaction between the burning glovebox and filter system have not been carried out.

In each of the glovebox experiments performed, the air temperature inside the burning box was measured by thermocouples. A plot of the time-temperature relationship for the two glovebox experiments is shown in Figure 10. The importance of these data are that they show the air temperature generated in a burning glovebox. These air temperatures set the conditions that must be countered for filter protection, since heat can cause loss of filter effectiveness.

A test has been made of the effectiveness of the water sprayed baffle in reducing the incoming air temperature. In this particular test, 6000 CFM of incoming air was heated to 1672°F and contacted the baffle. The massive baffle structure acts as a heat sink as well as promoting turbulence in the upstream plenum section. Without the water spray on, an air film heat transfer coefficient of $\frac{14.5 \text{ Btu}}{\text{Hr. ft}^2 \text{ °F}}$ was

FIGURE 8

Filter - holding frame

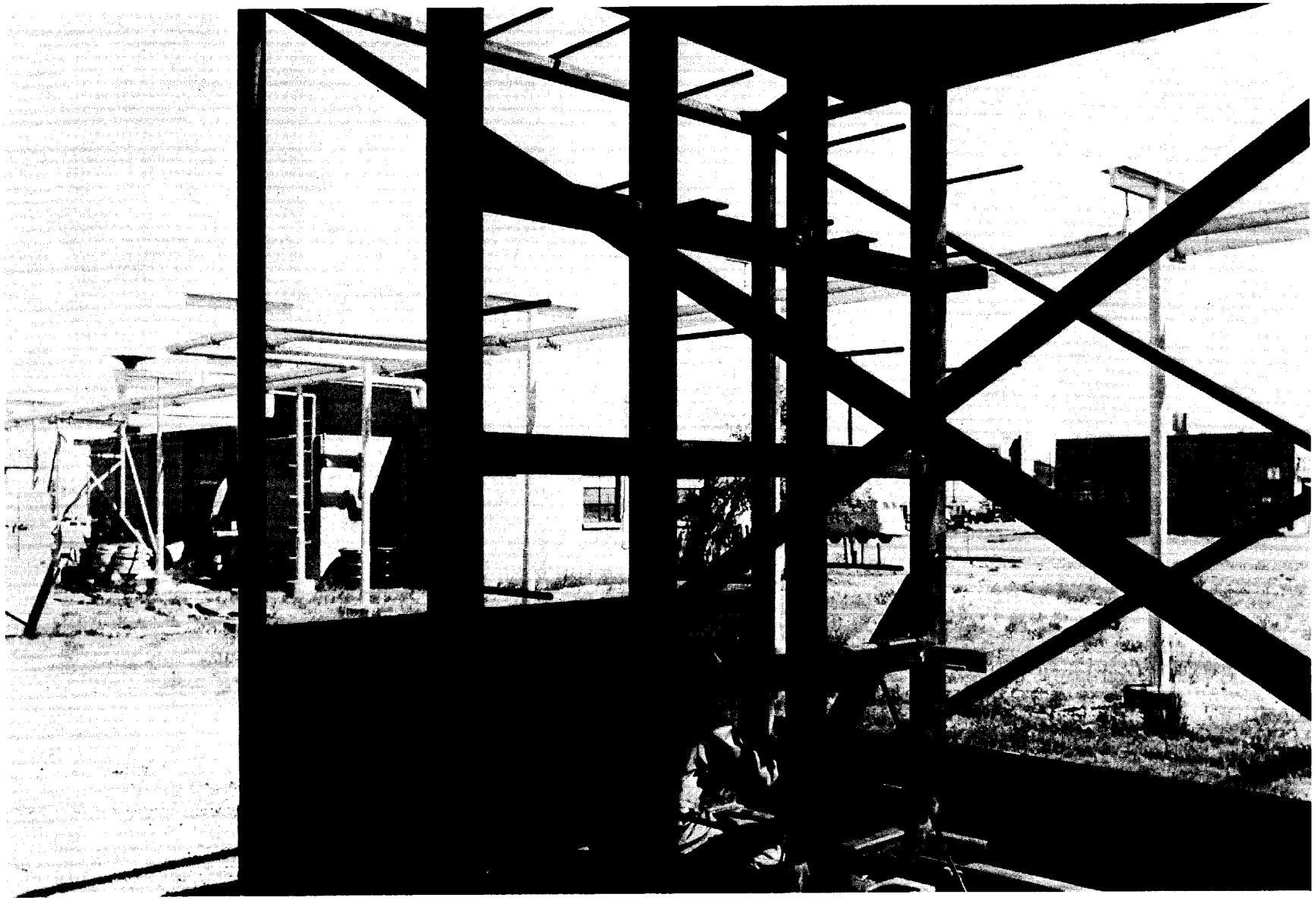

FIGURE 9

Detail of filter holding frame

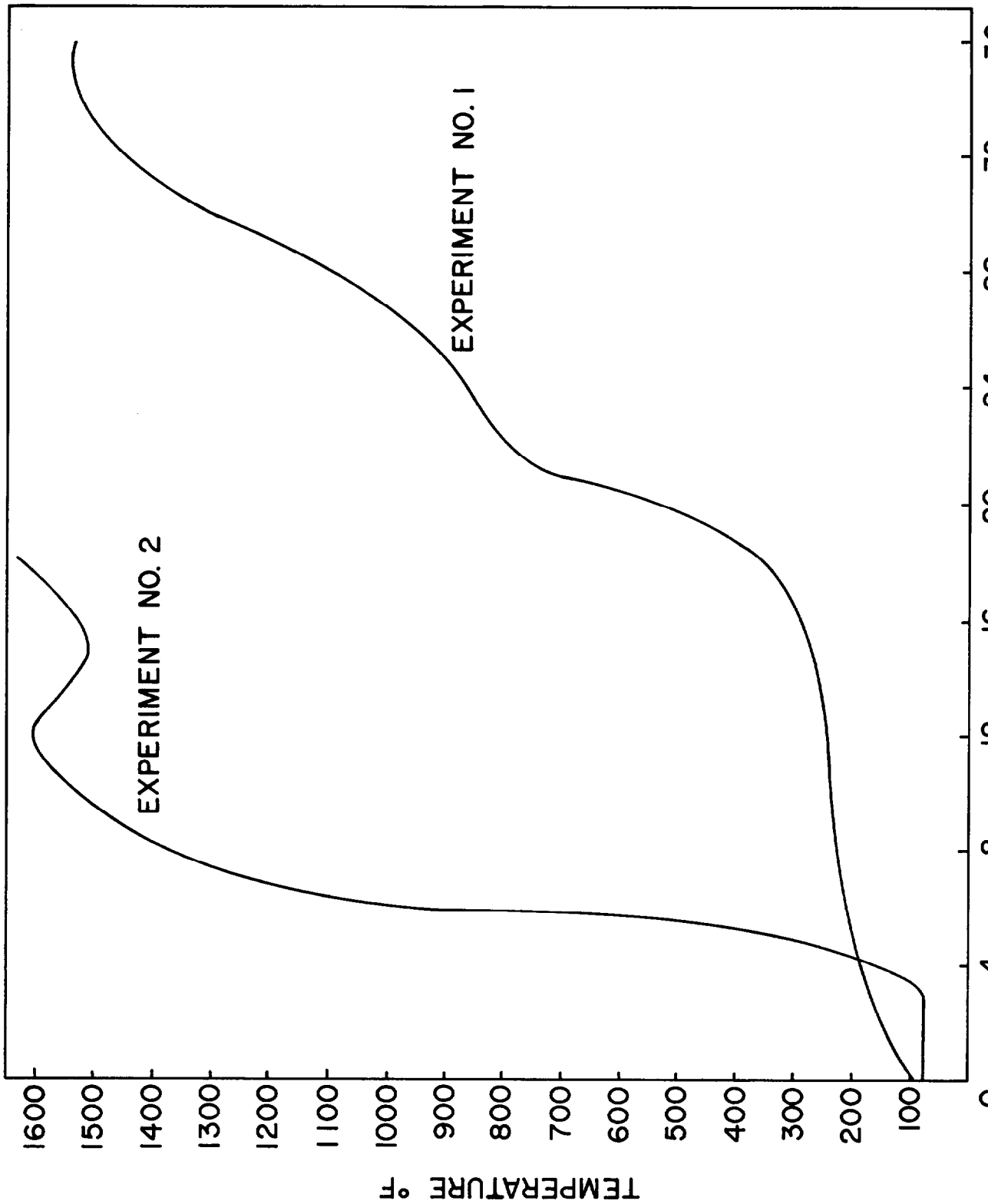

Figure 10 Air Temperature - Glovebox Burning Experiments

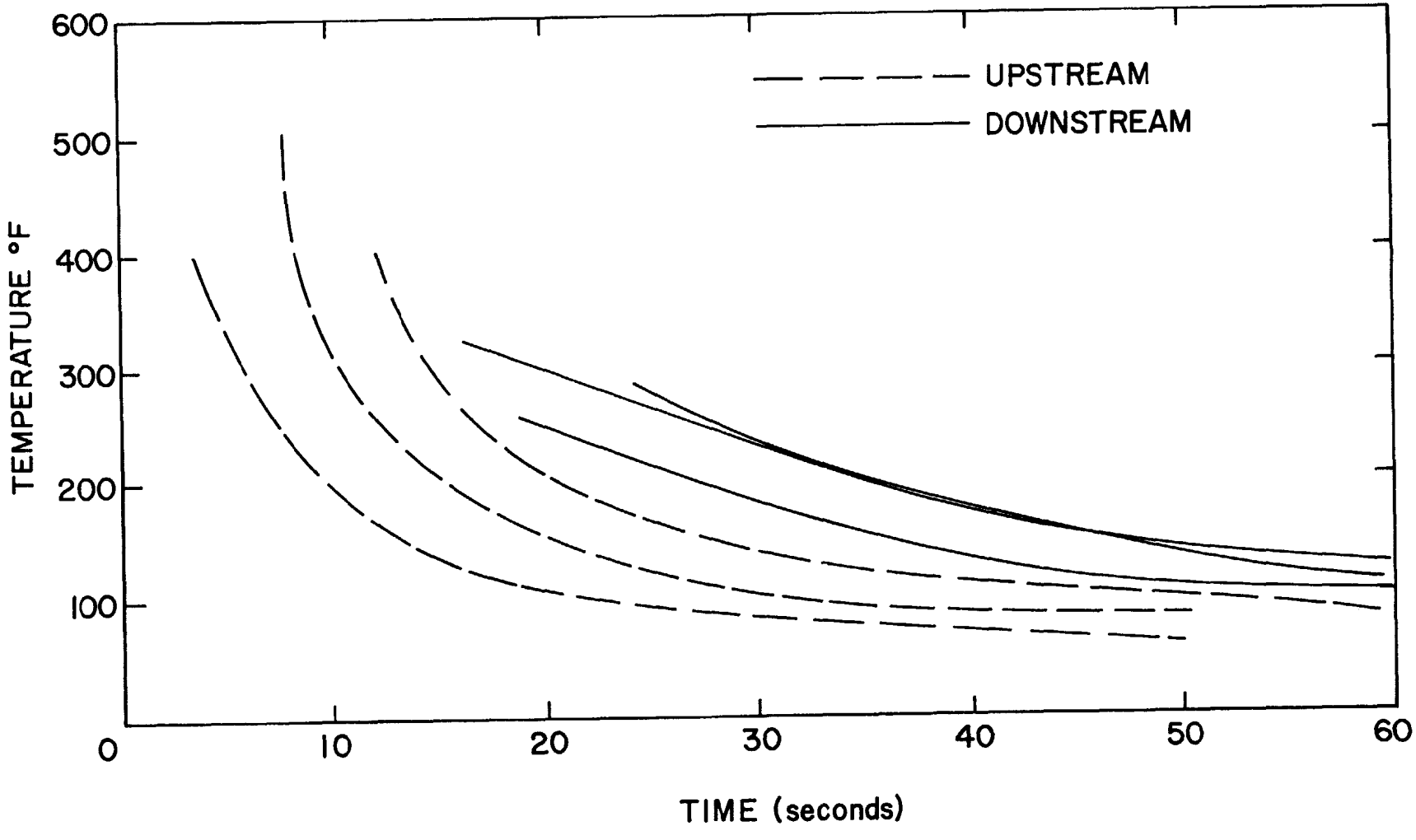

Figure 11 Performance of Water Spray-Cooled Baffle

calculated. With the water spray on, at a rate of 80 GPM, the water-air heat transfer coefficient was calculated to be 31.3 $\frac{\text{Btu}}{\text{Hr. ft}^2 \cdot ^\circ\text{F}}$. Figure 11 shows air-temperature plotted as a function of time, with the spray actuated at time zero. The upstream temperature drops more rapidly because the thermocouples were in the spray field. The downstream air temperature dropped to 125°F in one minute; therefore, the water spray baffle appears to be a very effective method of filter protection.

CARBON ADSORBER FIRE EXTINGUISHMENT TESTS*

Jack L. Murrow

Hazards Control
Lawrence Radiation Laboratory, University of California
Livermore, California 94550

ABSTRACT

Activated-carbon adsorbers in air-cleaning systems should be protected from fire. However, as they can ignite under unusual conditions, an adequate extinguishing system should be installed ready for use. This study examines some available systems.

The Savannah River-style cell (24 × 24 × 12 inches), containing approximately 60 pounds of 6-14 mesh carbon, was used for these tests. Single-head spray nozzles and arrays delivering up to 36 gallons per minute (gpm) at operating pressures to 150 psig, with patterns from fog to solid cone were tried using plain water and water with wetting agent. Under the conditions of this test, water sprays did not extinguish the fire as long as air continued to flow.

Liquid nitrogen was used successfully as an extinguishing agent under the same conditions. The rate of application to a single adsorber was 20 liters per minute for seven minutes.

Introduction

FIRE!

Such an alarm means trouble for everyone. To personnel responsible for the air-cleaning system installed in a building housing radioactive materials, fire can mean loss of occupancy for a prolonged period or contamination of the surroundings—a far greater problem in urban areas. This report deals with the problem of fire in the last component of high efficiency air-cleaning systems—activated-carbon adsorbers.

In 1966, E. I. duPont Co. (Savannah River Plant) asked us to verify laboratory ignition-point tests on activated charcoal. We tested a full size Savannah River-type adsorber for ignition point in our facility

*Work performed under the auspices of the U.S. Atomic Energy Commission.

for testing HEPA filters at high temperatures. Our fire department personnel were standing by; however, they failed to quench the ignited adsorber with CO_2 even though 495 pounds were used. Extinguishment was finally accomplished with water immersion. On later ignition point tests, the fire was satisfactorily extinguished by applying water at 7.5 gpm directly to the fire area with a solid-cone square-pattern nozzle attached to a wand.

Last year, we started a series of tests to determine optimum characteristics of an installed sprinkler system for extinguishing fires in multiple-cell carbon adsorber systems. Various nozzles were gathered, with delivery capabilities ranging from less than one to more than 18 gpm at pressures up to 150 psig. Figure 1 shows the nozzles tested.

Method

We standardized test conditions to permit meaningful comparisons. For these tests, Mr. Gilbert of AEC Health and Safety Div., Washington, D.C., furnished refurbished adsorber cells which had been loaded from a single batch of activated charcoal to ensure common burning characteristics.

The top left quadrant, looking downstream, was instrumented by inserting 5 iron-constantan thermocouples in the inlet side and 5 in the discharge side. The nozzle system was set up outside the test rig to check the size and completeness of coverage for a 24- by 24-inch area. The nozzle was then placed in the test rig at the distance determined.

The test sequence consisted of preheating the apparatus to 400°F, igniting the instrumented area with a torch, permitting a two-minute preburn to simulate detection delay, and starting the water spray. At ignition plus six minutes, external heat was removed. The progress of extinguishment was followed by observing through view ports upstream and downstream and by watching the temperature indicators.

Results

The results were disappointing. As shown in Table I, a variety of nozzles, with varied spray patterns, volumes, pressures, and additives, were unsuccessful under the test conditions. After several minutes of spray time, when test failure was certain, we had to terminate the test.

Repeated stopping and starting of the air flow while leaving the water spray on can extinguish the fire. However, even when the thermocouples indicate extinguishment, the fire may rekindle from a small hot spot if water is discontinued and air flow remains constant.

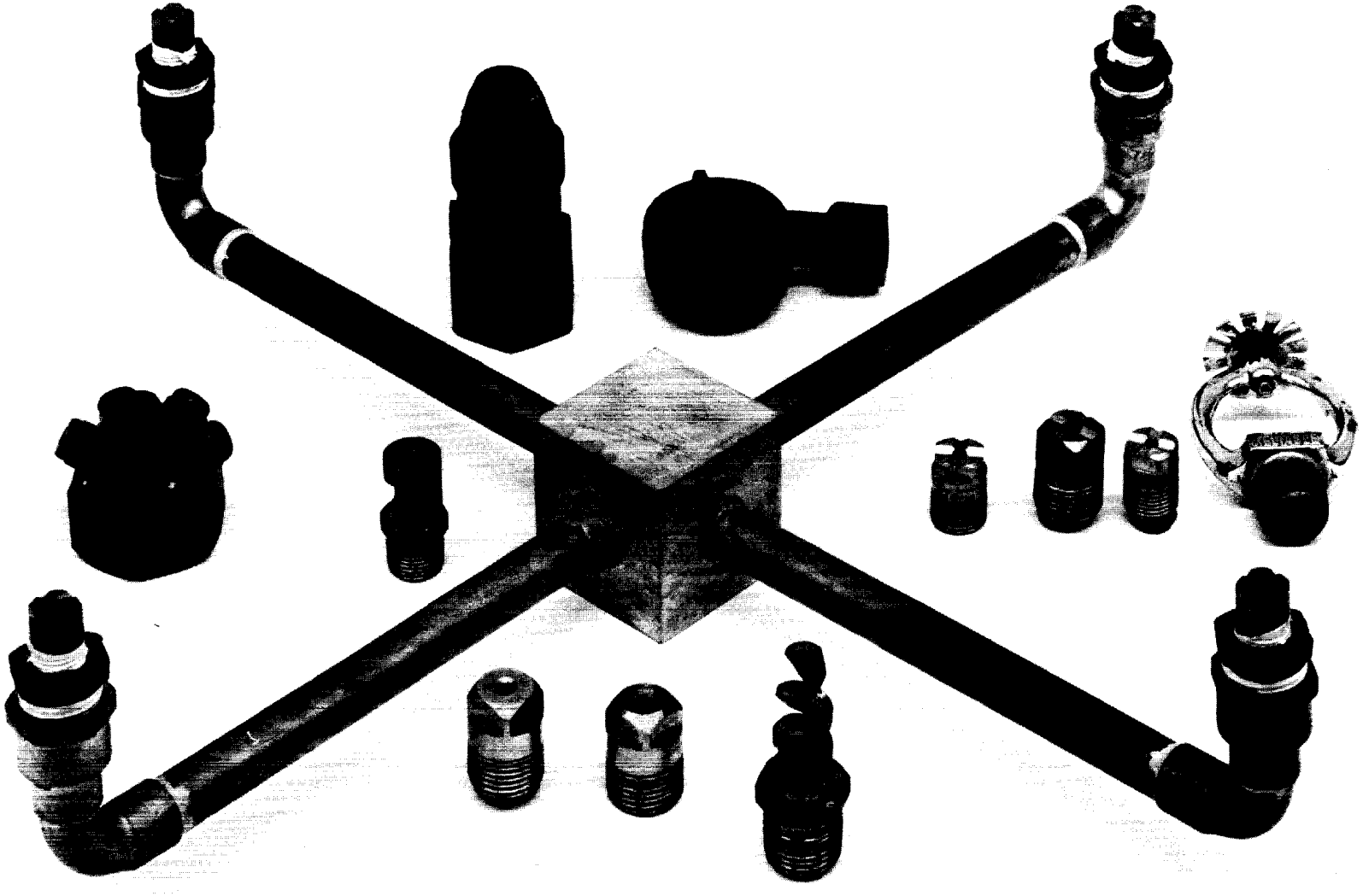

Fig. 1. Nozzles used.

Table I. Spray nozzles used and their characteristics.

Experiment No.	Nozzle Make	Model	Spray Characteristics	Remarks	Flow (gpm)	Back Pressure (psig)	Distance, Nozzle to Adsorber (in.)
69-10	Spraying Systems	3/4 7G-5	Multijet, Fog		4.8	20	25
69-11	Spraying Systems	1/2HH29 SQ	Square-solid cone		6.5	5	25
69-12	Spraying Systems	1/2HH 35W	Round-solid cone		7.5	48	15-1/2
69-13	SPRACO	Fire Fog #668WA	Round-solid cone		13	20	11
69-14	SPRACO	Fire Fog #668WA	Round-solid cone	One upstream - one downstream	13 ea.	20	11
69-15	SPRACO	Fire Fog #668WA	Round-solid cone	One upstream - one downstream	18.4 ea.	50	11
69-16	SPRACO	Fire Fog #668WA	Round-solid cone	One upstream-one downstream; solvoid wetting agent at 1 gal/ 1000 gal.	18.4 ea.	50	11
69-17	Spraying Systems	1/2HH29 SQ	Square-solid cone	W/solvoid wetting agent at 1 gal/1000 gal.	6.5	15	26
69-18	Spraying Systems	1/2HH 35W	Round-solid cone		7.5	20	11
69-19	Spraying Systems	1/2HH 35W	Round-solid cone		7.5	20	10-1/4
69-20 } 69-21 }	Spraying Systems	1/2HH29 SQ	Square-solid cone	4 nozzle array one nozzle at center of each quadrant.	7.5	2	11-1/2
70-22	Spraying Systems	1/4HH12 SQ	Square-solid cone	4 nozzle array, one nozzle center of each quadrant 1000 scfm - 10 sec 200 scfm - 20 sec	7.5 total	45	14
70-23	Spraying Systems	1/2HH29 SQ	Square-solid cone	same as above	10	5	15-1/4

Table I (cont'd)

Experiment No.	Nozzle Make	Model	Spray Characteristics	Remarks	Flow (gpm)	Back Pressure (psig)	Distance, Nozzle to Adsorber (in.)
70-24 70-25 70-26	Fabricated	—	Square pattern	Liquid nitrogen	5.3 (20 LPM)	35	13-1/2
70-27	Spraying Systems		Solid cone	24 - 4 per each of six pleats	3.5 total	40	3/4

The above manual method of extinguishment gave rise to another series of tests. An air-cylinder-actuated slide valve was installed in the system just upstream of the exhauster. "On" and "off" times could be set for desired periods, and a stop could be adjusted to prevent complete closure of the valve. This permitted tests to be run with flow variation (e.g., 1000 cfm for 10 seconds and 200 cfm for 20 seconds), which simulated an actual situation where the exhaust system needed to be reduced to assist the extinguishment, rather than being completely shut off. It did help, but complete extinguishment still did not occur.

Failure on every test of installed water systems made a different approach necessary. We decided to try liquid nitrogen (LN) because of two of its properties—cooling effect and inerting. However, our Maintenance Machinists found that some regular water-spray nozzles did not produce a spray with LN. They built the nozzle shown in Fig. 2 to solve the problem.

Figure 3 shows the system for introducing the liquid nitrogen. A pressure of 35 psig of nitrogen was sufficient to discharge the contents of the Dewar (about 150 liters) in seven minutes. The LN method was tried three times, and was successful each time. The preheat and preburn times were the same as for the water spray tests. Of course, a delivery rate of 20 liters per minute of completely vaporized liquid amounts to about 500 cfm, which halves the exhaust rate temporarily. There is no reignition if the cell is thoroughly chilled, an added bonus.

Observations, Suggestions and Plans

During some tests, a "sheath" of steam appeared to surround the jet of flame issuing from the cell. High-speed movies were taken in an effort to study this phenomenon, but it did not develop during the movie sequences. I believe it is caused by a small amount of water getting to the fire and turning into a steam cushion which prevents water from penetrating sufficiently to extinguish the fire.

The high-speed movies did show one phenomenon not observed visually. When the water hits the hot charcoal, there is a momentary flare-up lasting about a second. This has not been investigated and its cause is not known.

The hand method of extinguishing used during ignition-point testing suggested an array of 24 nozzles, four in each of the six pleats on the upstream side of the cell. A single test with 0.12 gpm per nozzle was unsuccessful. At preparation time for this paper further tests with larger nozzles have not been made. It is hoped that the results can be presented at the reading of the paper.

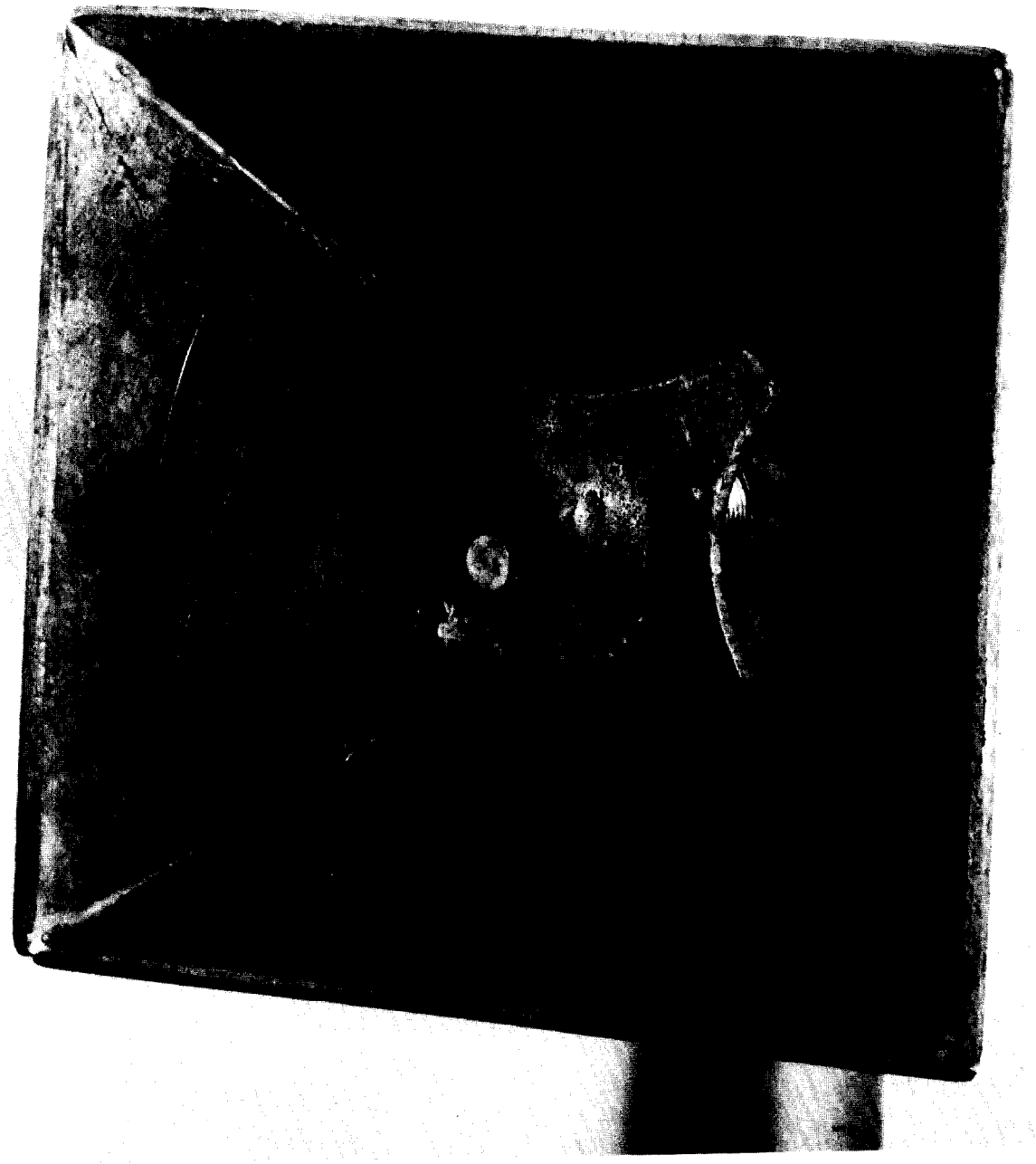

Fig. 2. Liquid Nitrogen nozzle.

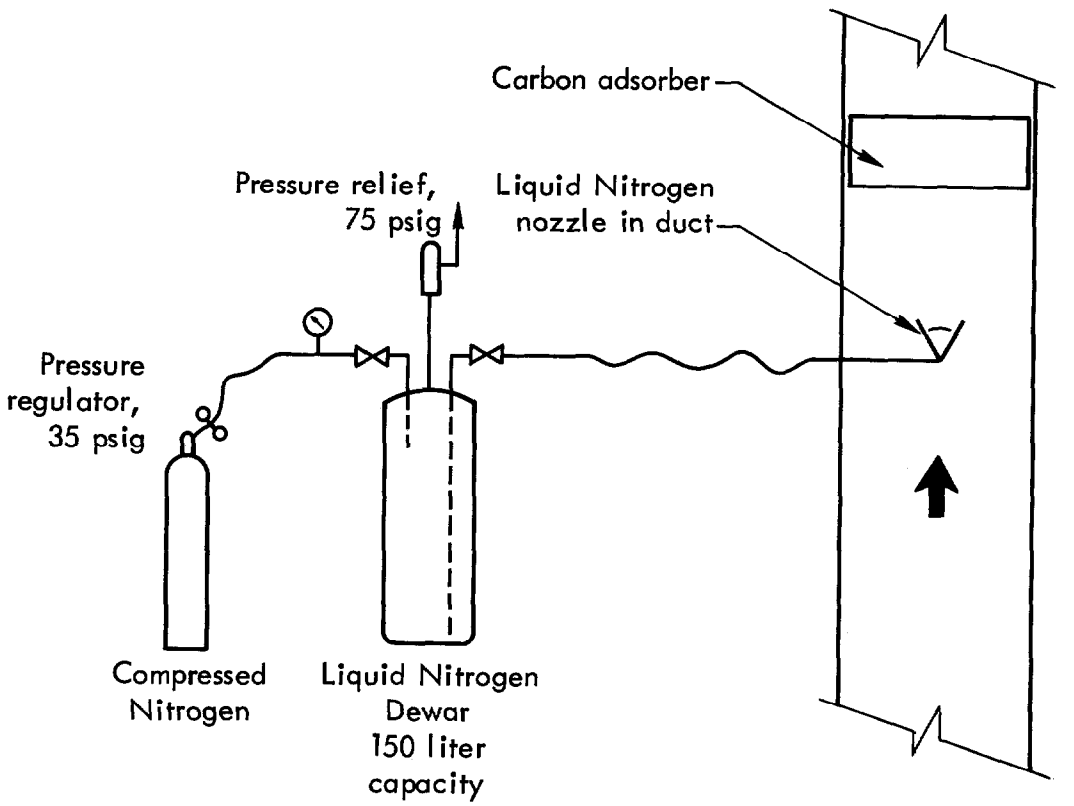

Fig. 3. Schematic, Liquid Nitrogen introduction.

Another method to be tried is the use of Halon 1301*. Portable hand extinguishers will be used to determine if the method has enough promise to warrant full scale tests.

Steam has also been suggested as a possible extinguishing agent. However, as no steam is available and our portable systems are too small, this method has not been tried.

Summary

Installed carbon adsorber banks must be protected from fire, whether caused by spontaneous ignition from radioactive decay, high organic chemical loading, or an external ignition source. However, installed sprinkler systems of reasonable gallonage have not yet been successful as fire extinguishers under the test conditions discussed.

Liquid nitrogen can be used as an extinguishing agent but must be readily available. Zone detection and extinguishment would be the only practical way for large installations.

Motion Picture

Following this presentation, Mr. Murrow showed the film:

"Savannah River Type Carbon-Adsorber/Fire Extinguisher Test by Water Spray," parts of which are commented on in the Open Discussion Session.

*Trademark - E. I. duPont Company.